sustainability

MDPI

Article

Eco-Friendly Synthesis of Silver Nanoparticles with Significant Antimicrobial Activity for Sustainable Applications

Ramona Plesnicute [1], Cristina Rimbu [2], Lăcrămioara Oprica [3,*], Daniel Herea [4], Iuliana Motrescu [5], Delia Luca [3], Dorina Creanga [1] and Marius-Nicusor Grigore [6]

1 Physics Faculty, Alexandru Ioan Cuza University, 700506 Iasi, Romania; plesnicuteramona@yahoo.com (R.P.); dorina.emilia.creanga@gmail.com (D.C.)
2 Veterinary Medicine Faculty, Ion Ionescu de la Brad University of Life Sciences, 700490 Iasi, Romania; cristina.rimbu@iuls.ro
3 Biology Faculty, Alexandru Ioan Cuza University, 700506 Iasi, Romania; luca_d2001@yahoo.com
4 National Institute of Research and Development for Technical Physics, 700050 Iasi, Romania; dherea@phys-iasi.ro
5 Horticulture Faculty, Ion Ionescu de la Brad University of Live Sciences, 700490 Iasi, Romania
6 Doctoral School of Biology, Alexandru Ioan Cuza University, 700506 Iasi, Romania; nicusor.grigore@uaic.ro
* Correspondence: lacramioara.oprica@uaic.ro

Abstract: Silver nanoparticles, with various uses in pharmacy, cosmetics, sanitation, textiles, optoelectronics, photovoltaics, etc., that are provided by worldwide industrial production, estimated to hundreds of tons annually, are finally released in the environment impacting randomly the biosphere. An alternative synthesis approach could be implemented by replacing chemical reductants of silver with natural antioxidants ensuring production and utilization sustainability with focus on environmental pollution diminishing. We synthesized silver nanoparticles by using plant extracts, aiming to offer antimicrobial products with reduced impact on the environment through sustainable green-chemistry. Fresh extracts of lemon pulp, blueberry and blackberry fruits as well as of green tea dry leaves were the sources of the natural antioxidants able to ensure ionic silver reduction and silver nanoparticle formation in the form of colloidal suspensions. The four samples were characterized by UV–Vis spectrophotometry, scanning electron microscopy, dark field optical microscopy, X-ray diffractometry, dynamic light scattering, which evidenced specific fine granularity, plasmonic features, standard crystallinity, and good stability in water suspension. Antimicrobial activity was assayed using the agar diffusion method and the bacteria kill-time technique against *Staphylococcus aureus* and *Escherichia coli*. In both cases, all silver nanoparticles revealed their adequacy for the aimed purposes, the sample synthesized with green tea showing the best efficiency, which is in concordance with its highest contents of polyphenols, flavones and best total antioxidant activity. Various applications could be safely designed based on such silver nanoparticles for sustainable chemistry development.

Keywords: silver nanoparticles; sustainable synthesis; antimicrobial activity; *Staphylococcus aureus*; *Escherichia coli*

check for updates

Academic Editor: Zhibin Ye

Received: 10 April 2025
Revised: 26 May 2025
Accepted: 4 June 2025
Published: 9 June 2025

Citation: Plesnicute, R.; Rimbu, C.; Oprica, L.; Herea, D.; Motrescu, I.; Luca, D.; Creanga, D.; Grigore, M.-N. Eco-Friendly Synthesis of Silver Nanoparticles with Significant Antimicrobial Activity for Sustainable Applications. *Sustainability* **2025**, *17*, 5321. https://doi.org/10.3390/su17125321

Copyright: © 2025 by the authors. Licensee MDPI, Basel, Switzerland. This article is an open access article distributed under the terms and conditions of the Creative Commons Attribution (CC BY) license (https://creativecommons.org/licenses/by/4.0/).

1. Introduction

Silver nanoparticles are widely used in medicine, pharmacy, sanitation, biotechnology, electronics, biosensors, agriculture and the food industry. Due to various applications in techniques and biomedicines, silver nanoparticle production is over 500 t annually [1].

Sustainable development involves several important aspects, such as increasing the percentage of energy obtained without fossil fuels as well as protecting the environment through industrial water purification. In this respect, because the efficacy of energy harvesting in solar cells could be enhanced by exploiting the surface plasmon resonance [2], some plasmonic solar cells with photoanodes incorporating AgNP fabricated by sustainable synthesis with banana extract were designed. Solar cell improvement was also demonstrated in [3], where silver nanoparticles were used in order to harness their plasmonic properties while silver nanoparticles in combination with luminescent molecules were designed as the basis of advanced heat transfer fluids, which are of real help in reducing electrical energy losses in photovoltaic systems [4].

Silver nanoparticles, due to their high surface/volume ratio, high selectivity, sensitivity, reactivity and especially their antibacterial characteristics, can be an alternative to water disinfection and microbial control [5], and moreover, to wastewater cleaning.

AgNPs synthesized with the plant species known as Persian cumin were shown to have catalytic properties when successfully tested to clean wastewater loaded with certain dyes namely nitrophenol, methyl orange, Congo red and methylene blue [6]. A similar effect on the same mentioned water pollutants was emphasized using silver/titanium dioxide nanocomposites prepared through green synthesis with the leaf extract of Mexican fireplant [7]. Due to their optical and electrical properties, silver nanoparticles can be used for the detection of aquatic pollutants at trace levels [8] allowing for the development of facile detection and analysis strategies with nanosilver-based electrodes [9].

Silver nanoparticles were shown to provide a real sensing ability of mercury by complexing it from heavy metal-polluted waters and allowing visual and quantitative spectral analysis based on the diminution of the intensity of the spectral band of non-complexed AgNPs [10]. Thus, riboflavin was used to conveniently modify AgNP surface aiming color contrast to the coupling of mercury [11] or even fluorescein, to also exploit fluorescence-based analytical techniques [12].

There are several main ways to prepare silver nanoparticles.

The physical methods are based on evaporation–condensation and laser ablation. Lee and Kang [13] reported that through thermal decomposition of silver oleate complexes silver ions are released which, in a nitrogen atmosphere at low pressure and high temperature, result in the formation of a silver crystallized nanopowder with a narrow-size histogram.

Boutinguiza et al. [14] demonstrated that spherical nanoparticles with narrow diameter distribution can be produced using polyol synthesis under nanosecond laser ablation in the open air and collected on glass support; however, for medical applications, they should be further prepared as aqueous suspensions. Tsuji et al. [15] reported that decreasing the laser wavelength could reduce the particle average diameter more than twice, up to 12 nm. The advantages of these synthesis methods are the high speed of production and the absence of toxic reagents using radiation as a reducing agent.

Chemical methods are mostly based on the reduction of silver nitrate, a low-cost and available salt precursor, requiring more affordable equipment and providing predictable results. Besides the most used reagents with a reducing capacity such as sodium borohydride [16]—suitable generally for small particle production and requiring a stabilizing agent—trisodium citrate—for silver particles with larger size distribution [17], other chemicals like mercaptoethanol, polyvinyl alcohol, hydrazine hydrate and thioglycerol can be utilized but whilst also considering their potential toxicity for applications in life sciences.

Green synthesis can be applied to AgNP production to minimize production costs and reduce the toxic impact on the environment where all the nanoparticles are finally released following their utilizations. Recent research found that biogenic AgNPs are less toxic than nanoparticles synthesized using chemical routes [18].

Therefore, the biological synthesis procedures developed in the last few decades are important as they consider the availability of silver ion reduction with bacteria [19–21], fungi [22–24] and some extracts from plant leaves and fruits [25–29].

Phytochemical synthesis of silver nanoparticles appears to be the most available method from the viewpoint of both natural antioxidant sources and costs. Much attention was paid to green tea leaves due to their rich content of polyphenols and flavones that made them preferable for daily use in many countries; therefore, they were considered as reducing agents for silver ion transformation to silver nanoparticles [30–33].

The benefits for the health of citric and tannic acids from lemons, limes and oranges were taken also into consideration for the phytosynthesis of silver nanoparticles with reduced cytotoxicity [34–39]. Furthermore, berries that are highly valued for their aroma and taste have been tested for their reducing capacity against silver ions like redcurrants [40], strawberries [41], blackberries [42], blueberries [43] and others.

The biomedical applications are based on silver's capacity to destroy microorganisms the main focus of our research is to evidence of the antibacterial activity of the silver nanoparticles yielded by phytochemical synthesis which was also the main objective of our study.

Thus, Ali et al. [31] evidenced the efficacy of AgNP synthesized with green tea against pathogen bacteria (*K. pneumoniae, S. aureus*, and *E. coli*) and *C. albicans* fungus, while Niluxsshun et al. [44] found that orange peel extract provided silver nanoparticles with remarkable antimicrobial activity against *S. aureus* and *E. coli*.

Silver nanoparticles synthesized with lemon zest extract [45] were found very efficient against *S. aureus, E. coli* and *C. albicans* while the phytosynthesis with strawberry and raspberry gave silver nanoparticles efficient against *S. aureus*, *E. coli*, *C. albicans* and other pathogen germs [46].

We present the results of our work regarding the antimicrobial activities of silver nanoparticles yielded with blueberries, blackberries, lemon and green tea, which were first characterized from the viewpoint of their physical–chemical features with focus on granularity and stability, thus proving they are promising products for biomedical applications.

2. Materials and Methods

2.1. Materials

Silver nitrate, methanol, sodium carbonate, sodium nitrite, gallic acid, catechin, aluminum chloride and sodium hydroxide were acquired from Sigma-Aldrich, 3050 Spruce Street, Saint Louis, MO, USA, while fresh fruits were purchased from commercial sources as well as dry leaves of green tea.

2.2. Silver Reduction with Lemon Extract

According to Dhulappanavar et al. [47] the pulp of lemon fruits, purchased from the commercial network was centrifugated at 5000 rpm for 15 min. A volume of 12.5 mL of the obtained supernatant was used for the reduction of 50 mL of 1 mM $AgNO_3$ solution. The mixture was heated at 80 °C under magnetic stirring (800 rpm) until the color changed to brown.

2.3. Silver Reduction with Green Tea Extract

We worked with an adapted version of the method of Nakhjavani et al. [48], mixing 7 g of dried green tea leaves crushed in a granite mortar with 400 mL of distilled water in an Erlenmeyer flask. The mixture was heated for 50 min up to approximately 60 °C being then boiled for another 10 min. After that, 5 mL of green tea extract was added to 50 mL 1 mM $AgNO_3$ in distilled water and heated for 5 more minutes at 40 °C under magnetic

stirring at 700 rpm. After cooling at room temperature, the mixture color changed from yellow to brown, indicating the formation of silver nanoparticles.

2.4. Silver Reduction with Blueberry Extract and Blackberry Extract

The synthesis was carried out according to the method of Li et al. [49], and Kumar et al. [50] by heating 5 g of fresh blueberry and blackberry fruits, respectively, in 50 mL of distilled water at 60 °C then mixing 5 mL of fruit extract with 50 mL of 1 mM $AgNO_3$ and continuing the heating at 60 °C under magnetic stirring at 700 rpm, for about 60 min, until the color of the mixtures turned to an orange hue.

2.5. Fruit Extract for Antioxidant Capacity Assay

Approximately 0.02 g of dried fruit samples were homogenized in 80% methanol and the mixture was stirred for 30 min then centrifuged at 3000 rpm for 15 min at 4 °C. The supernatant was used for subsequent determinations.

2.6. Total Polyphenol Content

According to Singleton et al. [51] the plant extract was mixed with Folin–Ciocalteau reagent and after 4 min, sodium carbonate, Na_2CO_3 15%, was added. A calibration curve was used that gives the light absorbance at 765 nm (Shimadzu PharmaSpec 1600 device, Shimadzu Corporation, Kyoto, Japan) after two hours, as a function of the gallic acid concentration. The total phenol content was expressed as milligram equivalent of gallic acid per gram of dry matter (mg GAE/g).

2.7. Total Flavone Content

Plant extracts in methanol and distilled water were used, and a solution of 5% $NaNO_2$ was added to each test tube. After five minutes, a 10% solution of $AlCI_3 \times 6H_2O$ was added and then, after six minutes, sodium hydroxide, NaOH 1.0 M was added too [51]. Finally, the test tube was filled with water under vigorous stirring [52]. The absorbance of the resulting pink solution was read at 510 nm against the control (distilled water). The flavone content was expressed as mg catechin equivalents per g of dry matter (mg CE/g).

2.8. Total Antioxidant Capacity

The DPPH free radical scavenging capacity was measured according to Molyneux [53]. Thus, 2 mL of 0.1 mM DPPH solution in methanol was mixed with 20 µL of methanolic extract of vegetal samples. The control (without any antioxidant) contains 80% methanol and DPPH solution. After 20 min the light absorbance at 517 nm was red and the percentage (%) of inhibition activity was calculated using the following Formula (1):

$$\% \text{ DPPH Inhibition} = (1 - \frac{A_E}{A_0}) \times 100 \quad (1)$$

where A_E is the absorbance of the sample with extract and A_0 is the absorbance of the DPPH solution in methanol.

2.9. Characterization Methods

Shimadzu PharmaSpec 1600 device was used to record spectral bands in UV–Vis domain, a specialized software being utilized to acquire and analyze the data.

An electron microscope STEM, type JEOL JSM 6390 (100 kV) (JEOL Ltd., Tokyo, Japan) was used to visualize the silver nanoparticles.

Dark field optical microscopy was applied with OPTIKA microscope in Dark Field mode, with 40× objective, and video camera and image capture software (OPTIKA Microscopes, Fino Mornasco, Italy).

XRD-X-ray diffractometry investigation was performed with Shimadzu Lab 6000 device (Shimadzu Corporation, Kyoto, Japan) with Kα (Cu) radiation having λ = 1.5406 Å. The diffraction angles were between 20 and 80 degrees in steps of 0.02 degree with scanning speed of 0.5 deg/min.

DLS—dynamic light scattering was applied using the MICROTRAC S3 500 device (Microtrac, Inc., Hatboro, PA, USA) to determine the size of suspended particles.

2.10. Antibacterial Activity of AgNPs on Bacteria

The antibacterial activity of AgNPs was tested using *Staphylococcus aureus* and *Escherichia coli.* These bacteria are categorized as healthcare-associated infections because of their potential to become human pathogens. The bacteria were grown on the agar plates at 37 °C overnight and after that, the bacteria were exposed to the AgNPs. The plates were monitored for changes after 24 h. For the analysis of antimicrobial activity, the diffusimetric method was applied [54]. The 24 h cultures of bacterial suspensions equivalent to the 0.5 McFarland standard (1.5×10^8 cfu/mL-cfu = colony forming units) were prepared from the standard strains *Staphylococcus aureus* ATCC 25923 (Gram-positive) and *Escherichia coli* ATCC25922 (Gram-negative), being inoculated in Mueller Hinton Agar (Oxoid) medium in sterile Petri dishes (Thermo Fisher Scientific (Oxoid), Waltham, MA, USA). A 10 µL of AgNP suspension taken as it was synthesized, with no further dilution, was pipetted over sterile filter paper discs (Ø6 mm), placed on the surface of Petri dishes, and the plates were incubated at 37 °C for 24 h. Also, the kill-time method was applied. In sterile Eppendorf tubes, 0.9 mL of microbial suspensions and 0.1 mL of AgNP suspension were let to interact. At 6-12-24-48-72 h, 100 µL of AgNP-treated bacterial suspension were distributed into sterile Petri plates, over which Mueller–Hinton Agar (Oxoid) medium was poured and let to melt and cooled to 45 °C, the plates being then incubated at 37 °C for 24 h. The number of colonies (cfu/mL—colony forming units/mL) was reported logarithmically to determine the percentage of logarithmic numerical reduction.

3. Results

3.1. Antioxidant Properties of Vegetal Extracts

The content of polyphenols in the four vegetal extracts utilized in this study in Figure 1 can be seen. The berry extracts presented rather similar polyphenol contents, of about 45 mg GAE/g for blueberries and 60 mg GAE/g for blackberries in the dry substance mass, while in the lemon pulp, approximately 20 mg GAE/g was found. The green tea leaf extract is characterized by a remarkably higher level of polyphenols—around 180 mg GAE/g—triple when compared to blackberries (standard deviation of about 5%), while the value of 89.4 mg GAE/g of green tea dry substance was found by Demirel Bayik, et al. [55].

In Figure 2 we present the results of flavone content assay expressed as catechin equivalent per gram of dry vegetal substance (standard deviation of 11%). In addition, the highest content of antioxidants for green tea was highlighted—about 27 mg catechin per gram of dry matter, compared to berries—with about 7.5 mg catechin per gram of dry matter and with lemon (about 2 mg catechin per gram of dry matter).

In Figure 3 the results of total antioxidant capacity expressed as DPPH free radical scavenging capacity are given.

We found similar antioxidant properties for green tea leaves and blackberry fruits of around 88% and 89%, respectively. For blueberry fruits, the DPPH free radical scavenging activity was estimated to be about 72% while for fresh lemon extract, about 36% was found (the standard deviation being 3.5%). In Figure 4 these results are summarized to compare the properties of the four plant extracts.

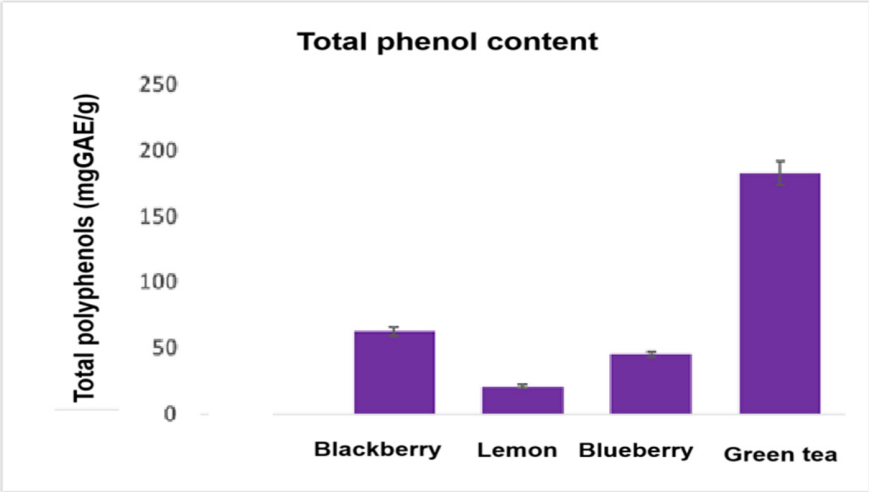

Figure 1. Total polyphenol content in the vegetal extracts.

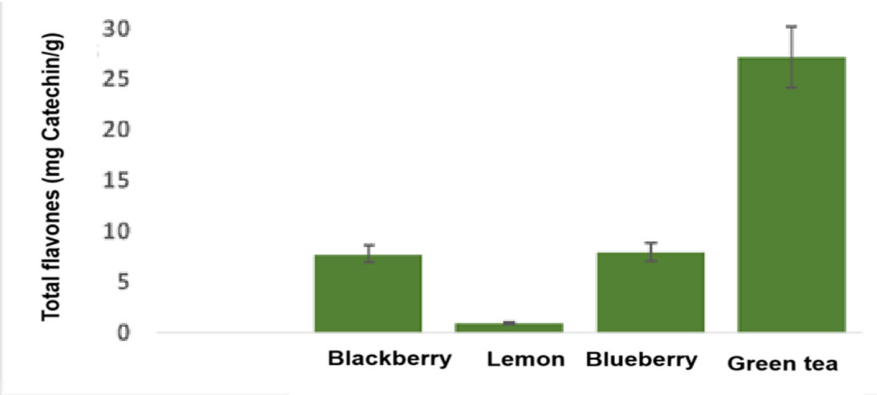

Figure 2. The flavone content in the studied vegetal extracts.

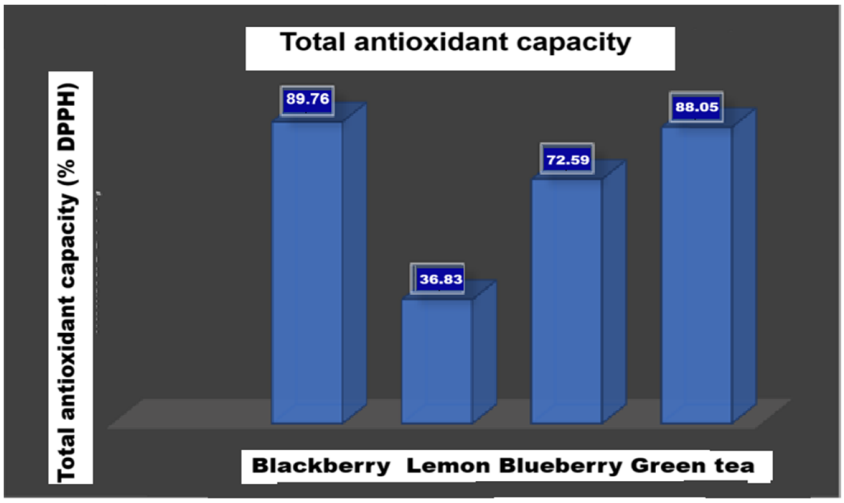

Figure 3. The total antioxidant activity of the vegetal extracts with DPPH method.

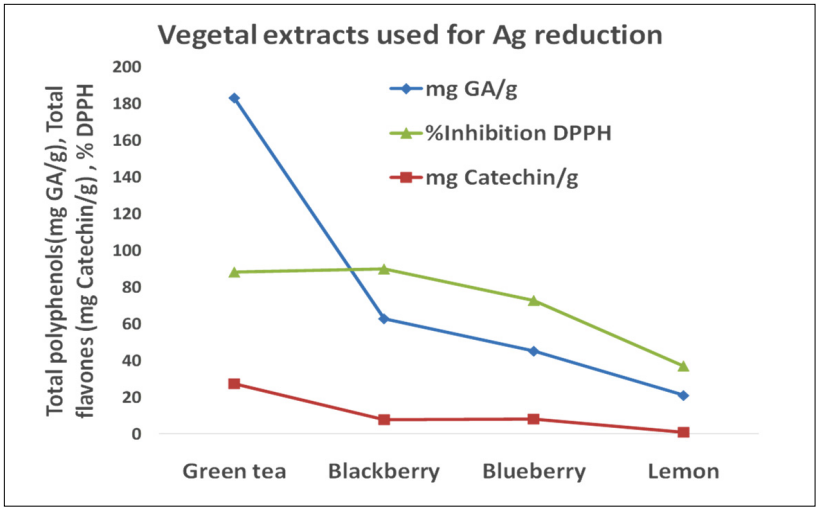

Figure 4. Comparison between the reducing properties of green tea leaves, lemon pulp, blueberry and blackberry fruits.

3.2. Spectral and Optical Characterization

The characteristic spectral band of silver nanoparticles was the first criterion in monitoring and assessing the formation of silver reduced with vegetal extracts. In Figure 5 we present the recorded absorption spectra in the visible and near UV range for the studied silver colloidal suspensions. In Figure 5 one can see the spectral band of AgNP–lemon, as a result of following the synthesis protocol, with maximum intensity at 425 nm and relatively wide shape denoting particle size polydispersity and the spectral band recorded in the visible range for AgNP–green tea, also large, presenting the absorption intensity stabilized at about 450 nm. The AgNP–blueberry samples have the maximum intensity at 458 nm when stabilized after 27 days of storage in darkness in a refrigerator while the silver nanoparticles synthesized with blackberry extract (AgNP–blackberry sample) presented the large width characteristic band at 429 nm after 14 days of storage in the darkness, in the refrigerator. A remarkably long time of stabilization—120 days—was reported by Lima et al. [56] for AgNPs synthesized with *Candida lipolytica* biosurfactant. Other reports described their similar results as can be seen in the text below.

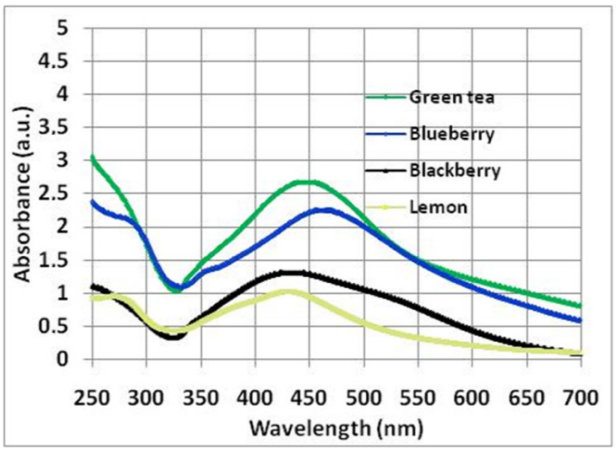

Figure 5. The spectral bands in the visible and near UV ranges of the silver nanoparticles synthesized with plant extracts.

The intensity in the maximum of the spectral bands, reflecting the ability of natural reducers to provide silver nanoparticles, varies as follows: green tea > blueberry > blackberry > lemon. The value for AgNP–green tea was the highest, as expected, given the

biochemical parameters that describe the reducing capacity are the highest for green tea extract. At the same time, the band of lowest intensity for AgNP–lemon is consistent with the lowest levels of polyphenol content, catechin content and antioxidant capacity (Figure 4), while for AgNPs synthesized with berries, the intermediate values of their maximum intensity in the spectral bands, are consistent with the intermediate values of biochemical parameters expressing reducing characteristics.

3.3. Results of Microscopy Investigation

In Figure 6, the particles imaged with SEM appear rather well dispersed, having symmetrical geometric shapes, mostly quasi-spherical, with diameters of tens of nm, similar to the data resulting from the optical microscopy investigation, in dark field mode.

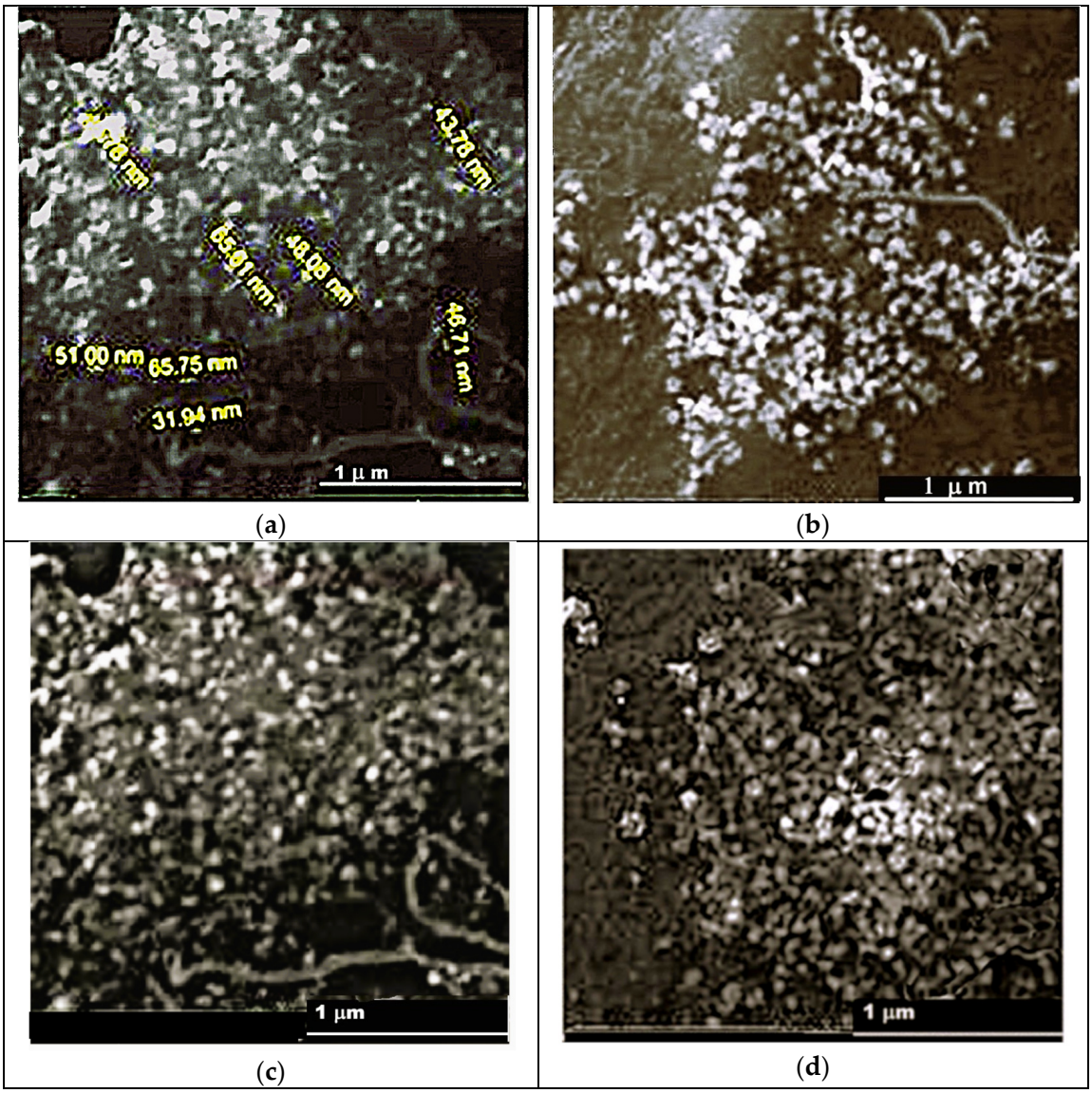

Figure 6. (**a**–**d**) The silver nanoparticles visualized with SEM technique: (**a**) AgNP–lemon, (**b**) AgNP–green tea, (**c**) AgNP–blueberry, (**d**) AgNP–blackberry.

According to SEM results, the AgNP–lemon suspension presents the most frequent particles with diameters of 35–65 nm (Figure 6a) while the AgNP–green tea sample is characterized by nanoparticles with mostly a 30–60 nm size (Figure 6b). The silver nanoparticles synthesized with berry extracts generally exhibit particles of 25–50 nm (AgNP–blueberry, Figure 6c) and 30–55 nm (AgNP–blackberry, Figure 6d). The next figures present the im-

ages captured with the optical microscope for AgNP samples synthesized by eco-friendly methods. For AgNP–lemon the diameters range between 15 and 40 nm (Figure 7a) while the AgNP–green tea sample presents diameter values of 15–55 nm (Figure 7b).

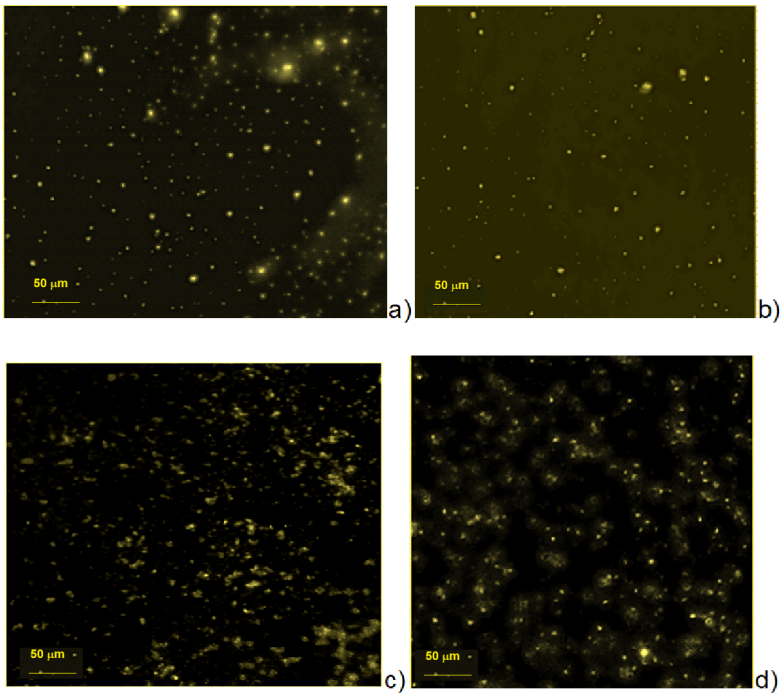

Figure 7. Results of dark-field optical microscopy analysis for: (**a**) AgNPs synthesized with lemon extract, (**b**) AgNPs synthesized with green tea extract, (**c**) AgNPs synthesized with blueberry extract, (**d**) AgNPs synthesized with blackberry extract.

The Dark Field microscopy method enables the estimation of the metal colloidal nanoparticles size due to the localized surface plasmon resonance, since the plasmonic image size is two orders of magnitude larger than that of the nanoparticles, being mainly determined by the source-emitter metal particles but including also the influence of the molecular shell electro-optical properties. ImageJ 1.54d version software with an image scale bar and microscope ocular scale calibration was utilized to read and collect the diameter range.

In Figure 7c,d the visualization of AgNP–blueberry and AgNP–blackberry is given with diameter found between 25 and 70 nm and 22 and 67 nm, respectively, and with some associations between neighboring nanoparticles mainly for AgNP–blueberry nanostructures (Figure 7c).

3.4. Results of Crystallinity Analysis

The crystallinity features of silver nanoparticles, investigated with the X-ray diffraction technique, are presented by means of the diffractograms in Figure 8a,b and Table 1.

According to Figure 8a–d, in the diffractograms recorded for the AgNP samples synthesized by us, all the diffraction maxima of cubically crystallized silver are found, the Miller indexes and the corresponding diffraction angles are given in Table 1.

According to JCPDS (Joint Committee on Powder Diffraction Standards file no. 04-0783), all four AgNP samples have dominantly the specific silver crystal structure, being occasionally accompanied by the maximum of oxidized silver (AgO, (JCPDS, file No. 84-1108)), very prominent in the case of the AgNP–lemon sample (Figure 8a) and possibly overlapped on certain maxima of organic crystals resulted from the synthesis procedure (denoted with (*)). Such maxima could be also present at other diffraction angles but,

because of their small intensity (corresponding to a small amount of organic crystals), they are comparable with the recording noise. An amorphous phase also appears, as seen in the low-angle range (20–30 degrees) for the AgNP–lemon sample corresponding to glass support.

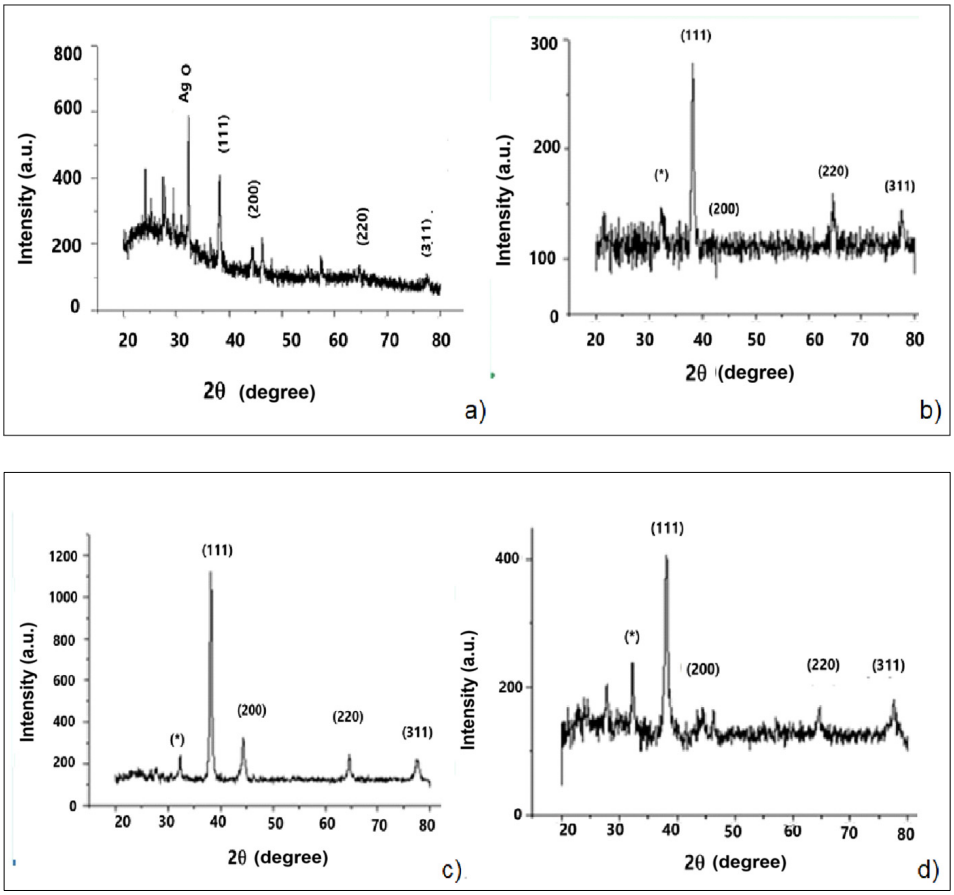

Figure 8. (**a**–**d**). XRD analysis results for: (**a**) AgNP–lemon, (**b**) AgNP–green tea, (**c**) AgNP–blueberry, (**d**) AgNP–blackberry. (*) organic crystals.

Table 1. The results of crystallinity investigation.

Miller Indexes (hkl)	(111)	(200)	(220)	(311)
AgNP–lemon				
2 θ (°)	38.15	44.38	64.54	77.41
AgNP–green tea				
2 θ (°)	38.16	-	64.56	77.49
AgNP–blueberry				
2 θ (°)	38.15	44.35	64.53	77.45
AgNP–blackberry				
2 θ (°)	38.16	44.32	64.50	77.43

We also mention that the background noise from the recording also became an impediment in determining the crystallite size for all the analyzed samples.

3.5. Results of Hydrodynamic Diameter and Zeta Potential Measurement

In Figure 9, the results obtained for the AgNP–lemon sample are graphically presented with the calculated D_h of 120 nm, and the polydispersity index, PDI = 0.11. This rather low value of the PDI parameter (below 0.3) describes a good monodispersity in the studied suspension. The Zeta potential (Figure 9b) of −2.88 mV indicates a very low charge at the colloidal particles that corresponds to a small contribution of the electrical repulsion to maintaining the particles well dispersed.

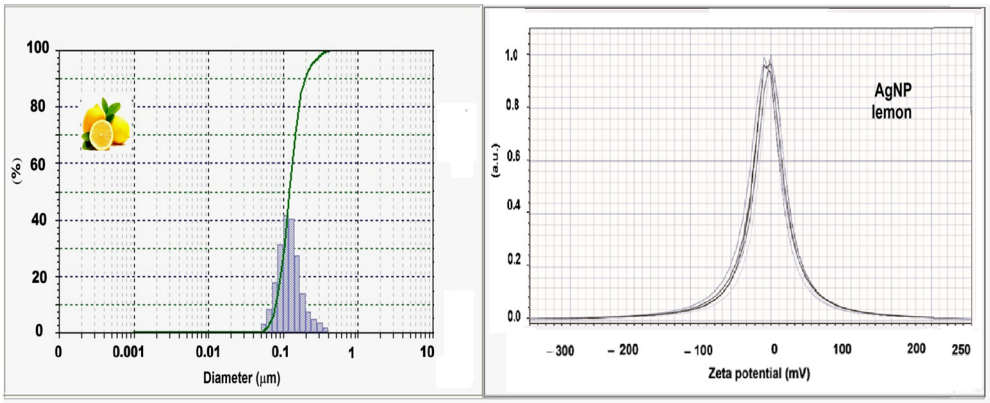

(**a**) (**b**)

Figure 9. (**a**) The hydrodynamic diameter and (**b**) Zeta potential for AgNP–lemon sample.

For the AgNP–green tea sample, a similar result was found as for AgNP–lemon, of 121 nm for the hydrodynamic diameter (Figure 10a), with good dimensional monodispersity, according to the small PDI index, of 0.13. Since the Zeta potential value is −4.33 mV (Figure 10b) it seems that the stability of the suspension is ensured mainly by steric forces in this case too.

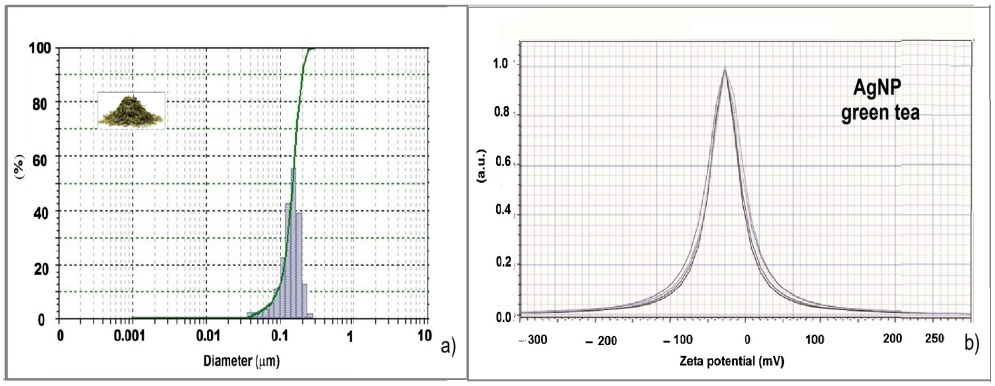

Figure 10. (**a**) The hydrodynamic diameter and (**b**) Zeta potential for AgNP–green tea sample.

From Figure 11a, the hydrodynamic diameter for the AgNP–blueberry sample, was found to be 61 nm while the PDI value was 0.29 (an index lower than 0.3 indicating good monodispersity). According to Figure 11b, the Zeta potential was −17.28 mV supporting the hypothesis that the electrostatic repulsion is relatively strong and has a more significant role in the stability of the suspension than in the two previous cases.

From Figure 12a, the D_h value was found at 67 nm and the PDI of 0.12 was obtained for AgNP–blackberry nanoparticles, while in Figure 12b, the Zeta potential can be seen, at−18.04 mV; therefore, it can be said that the two suspensions prepared with berries behave similarly, and the hydrodynamic diameter is close to those provided by SEM and dark-field optical microscopy.

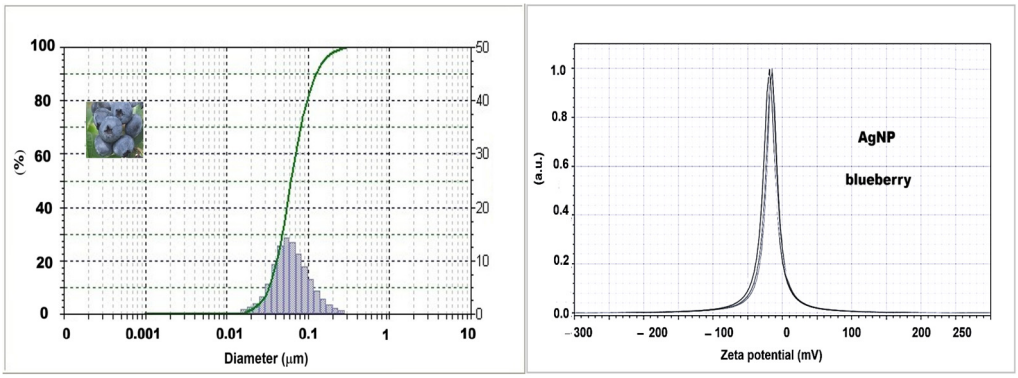

(**a**) (**b**)

Figure 11. (**a**) The hydrodynamic diameter and (**b**) Zeta potential for AgNP–blueberry.

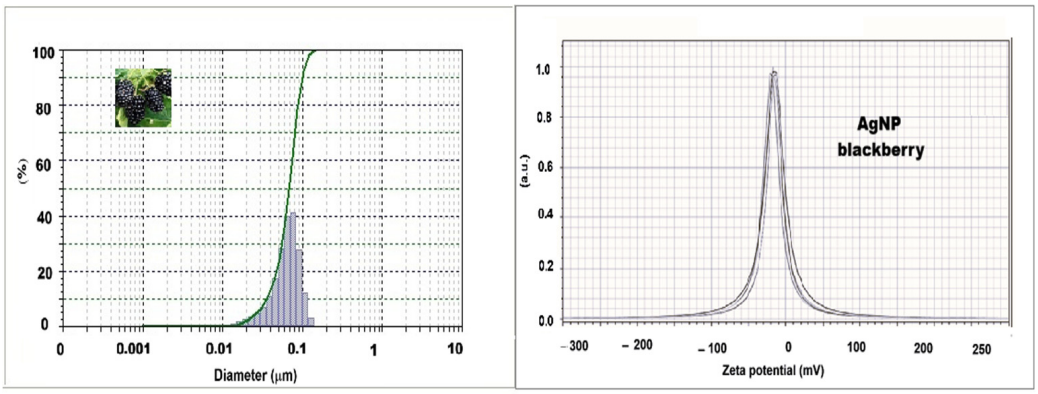

(**a**) (**b**)

Figure 12. (**a**) The hydrodynamic diameter and (**b**) Zeta potential for AgNP–blackberry.

In Figure 13, the size distributions of the four AgNP samples are compared, and it is not difficult to observe that the hydrodynamic diameters for the synthesis with berries (blueberries and blackberries) are the smallest.

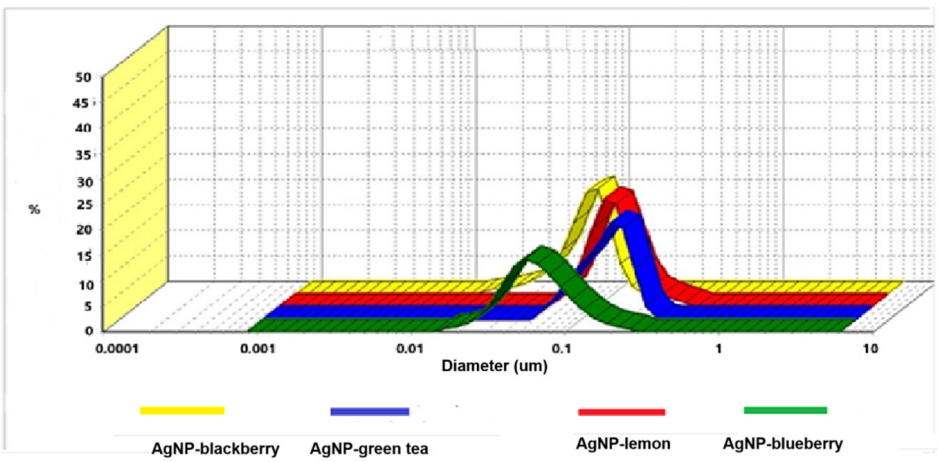

Figure 13. Comparison between the hydrodynamic diameters obtained for AgNP samples synthesized with plant extracts.

3.6. The Results of Antimicrobial Activity Tests

3.6.1. The Results of Agar Diffusion Method Application

In Figure 14a–d, some photographic images of the Petri dishes showing the zones of microbial growth inhibition can be seen. Thus, in Figure 14a,b, the largest zones of

S. aureus growth inhibition can be seen around the C-sample (for AgNP–green tea) while the smallest antimicrobial activity revealed by this method was evidenced for the AgNP–lemon sample ($^{m}L^{m}$-sample). In the case of *E. coli*, the largest growth inhibition zones were found for the suspensions of AgNP–blackberry and AgNP–lemon (notations: A^{m} and $^{m}L^{m}$ on Figure 14c,d).

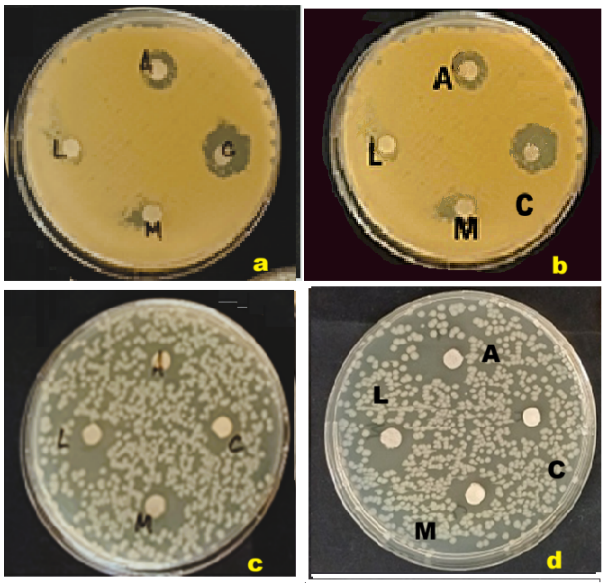

Figure 14. (**a**–**d**) Images of Petri dishes with zones of microbial growth inhibition for: *S. aureus* (**a**,**b**) and *E. coli* (**c**,**d**). (A—Blueberry; L—Lemon; M—Blackberry; C—Green tea).

It seems that the diffusion of the nanoparticle suspension occurred less isotropically than for certain molecular solutions of antibiotics, for instance, because particles are much larger than molecules and their mobility is lower and also because unlike the molecules in a solution (that are all equal in size and volume), the nanoparticle suspensions are characterized by size polydispersity.

Indeed, as presented above, the spectral bands in visible and near UV range through their relatively large width denote the AgNP suspensions' polydispersity. Thus, the inhibition zones appear less regular than the circular areas obtained for other inhibitory agents of a molecular nature like solutions of antibiotics. Also, in the case of *E. coli*, the microbial growth that was revealed by applying the described antimicrobial assay consists of not quite uniformly spread colonies that contribute to the irregularities in the shape of the growth inhibition zones (Figure 14c,d).

According to Figure 15, for the *S. aureus* bacterium, the highest average diameter of over 15 mm of the translucent zones with growth inhibition around the disks soaked with silver nanoparticle suspension was revealed for theAgNP-green tea sample; then, a 10.5 mm average diameter was obtained for AgNP–blackberries, a 7.5 mm average diameter was evidenced for AgNP–blueberries while the smallest value of 7.5 mm corresponds to AgNP–lemon.

In the case of *E. coli*, the largest average diameters were obtained for AgNP–lemon and AgNP–blackberry (18.5 mm in both cases) while for the other two silver suspensions, 11.0–11.5 mm diameters were obtained (Figure 15).Thus, the higher susceptibility of *E. coli* compared to *S. aureus* to the action of the antimicrobial silver nanoparticle suspensions was illustrated.

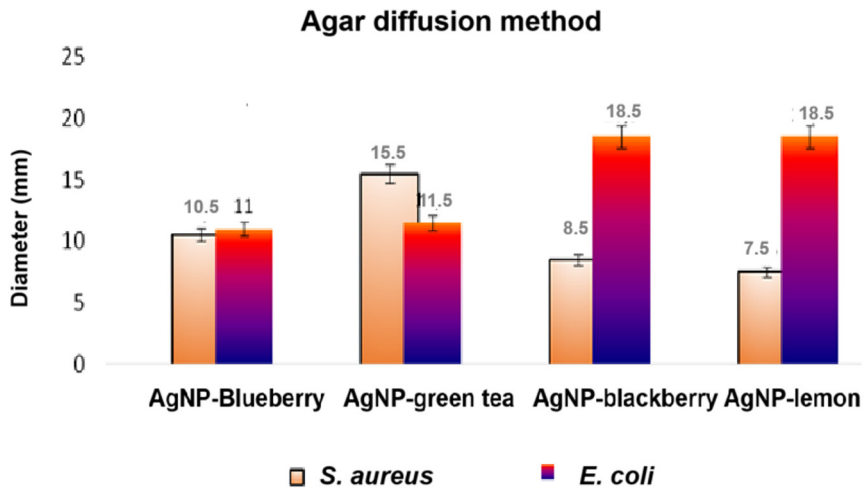

Figure 15. Results of the diffusimetric method for the pathogenic germs tested.

3.6.2. The Results of the Kill-Time Test Application

The images in Figure 16a–h show the surface of the Petri dishes with the microbial colonies for each of the five chosen interaction times. The results are shown for two repetitions of the experiment. The average values were used for graphical representation and for interpretation of the results.

For each of the eight cases (Figure 16a–h), the values found for LogN/mL were represented on the comparative graphs in Figures 17 and 18. The higher the antimicrobial activity of an AgNP sample, the shorter the reduction to zero of the number of microbial cells.

In Figure 17, we can see the killing times obtained for *S. aureus* according to the data processing in Figure 16a–d. In each case, the number of viable microorganisms is expressed logarithmically (Log N/mL) where N is the concentration of microbial cells per mL of culture medium inoculated and treated with AgNP particles.

For the AgNP samples synthesized with berry extracts (blueberries and blackberries), we achieved a 24 h killing time (AgNP–blueberries) and a 48 h killing time (AgNP–blackberries) for *S. aureus* germs. Relatively high levels of microbial density were revealed for the first observation time of 6 h (Figure 17), namely 36,270 for AgNP–blueberries and 41,000 for AgNP–blackberries (Figure 17).

However, significantly higher efficiency against the *S. aureus* bacterium was found for the AgNP–green tea and the AgNP–lemon samples, which completely destroyed the microbial cells after 24 h of interaction, starting from considerably lower levels at the time of observation at 6 h, i.e., logN/mL equal to 510 for AgNP–green tea and 710 for AgNP–lemon. This is concordant with the results of the agar diffusion test, where the AgNP–green tea sample led to the largest zone of *S. aureus* growth inhibition.

In Figure 18 we can see the killing times obtained for *E. coli* from the processing of the data of Figure 16e–h. Initially, the survival of *E. coli* cells after the first 6 h of interaction with silver nanoparticles is given by the values of LogN/mL of 4680 (AgNP–lemon), 1430 (AgNP–blackberry), 910 (AgNP–blueberry) and 30 (AgNP–green tea). After 24 h, the microbial growth corresponding to the AgNP–blackberry sample is zeroed, and after 48 h, the values corresponding to the AgNP–blueberry and AgNP–lemon samples are also reduced to zero.

The AgNP–green tea sample destroys the microbial growth of *E. coli* germs after only 12 h, making it the most effective of the four samples we studied.

Also, considering the results in Figure 15, it seems that the efficiency of the silver nanoparticles studied in this research is higher for *E. coli* than for *S. aureus*, as the destroying

of microbial growth occurs at shorter times while the zones of inhibition of microbial growth have generally larger diameters.

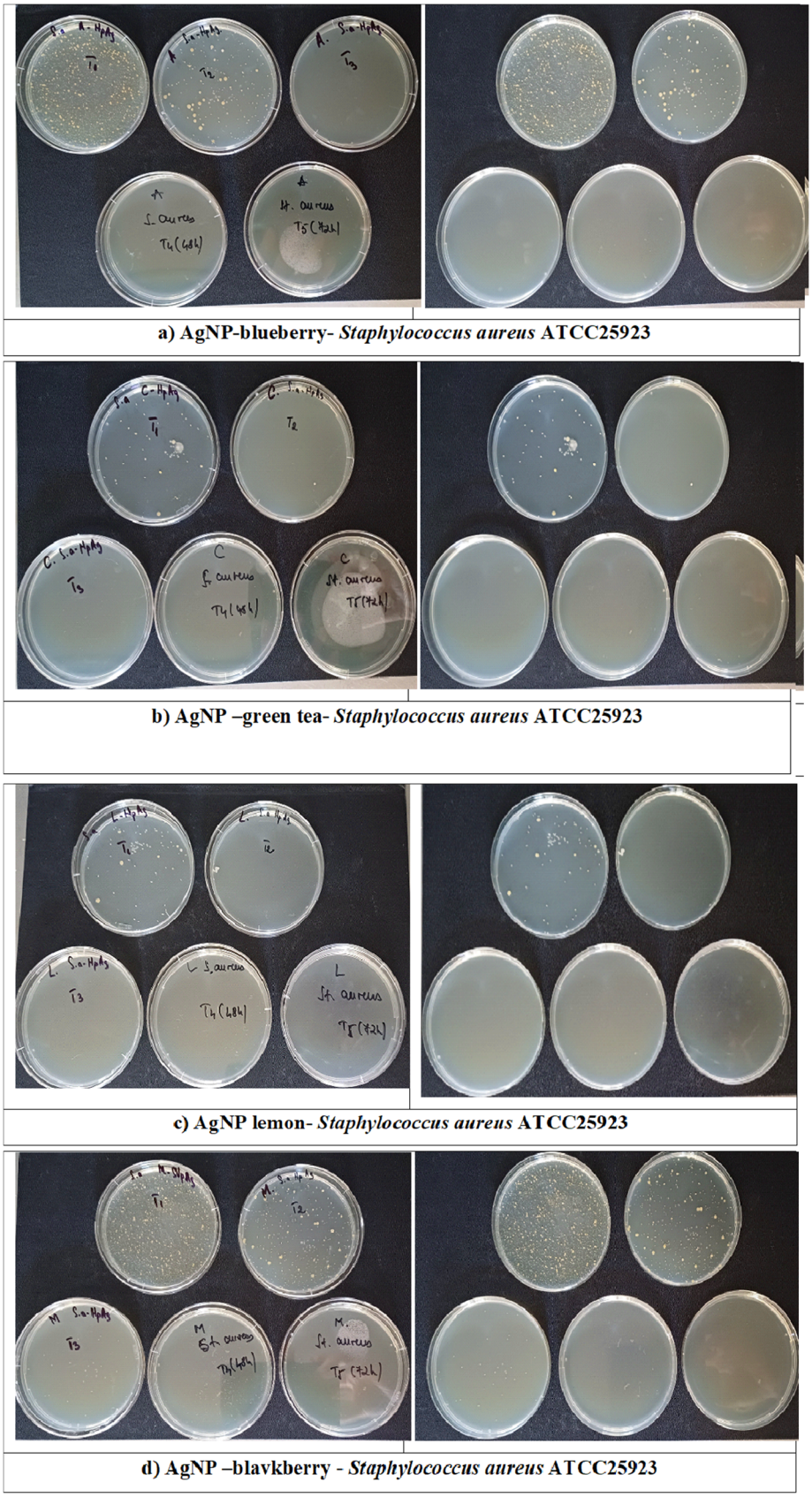

a) AgNP-blueberry- *Staphylococcus aureus* ATCC25923

b) AgNP –green tea- *Staphylococcus aureus* ATCC25923

c) AgNP lemon- *Staphylococcus aureus* ATCC25923

d) AgNP –blavkberry - *Staphylococcus aureus* ATCC25923

Figure 16. *Cont.*

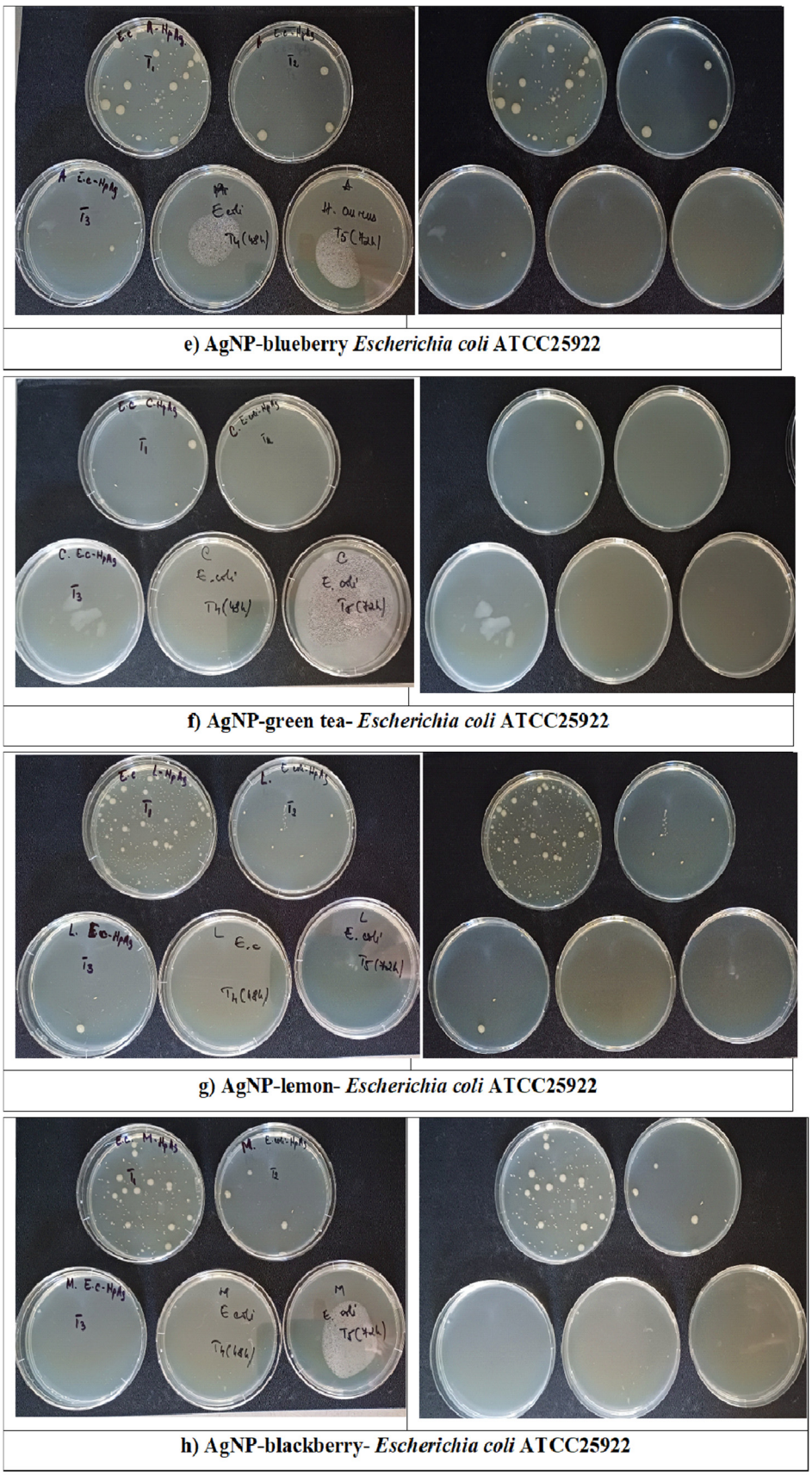

Figure 16. (**a**–**h**) Photographic images at 6, 12, 24, 48 and 72 h with the microbial growth of *Staphylococcus aureus* ATCC 25923 (**a**–**d**) and *Escherichia coli* ATCC25922 (**e**–**h**) germs, exposed to the samples of AgNP–blueberry, AgNP–green tea, AgNP–lemon and AgNP–blackberry, tested by the kill-time technique.

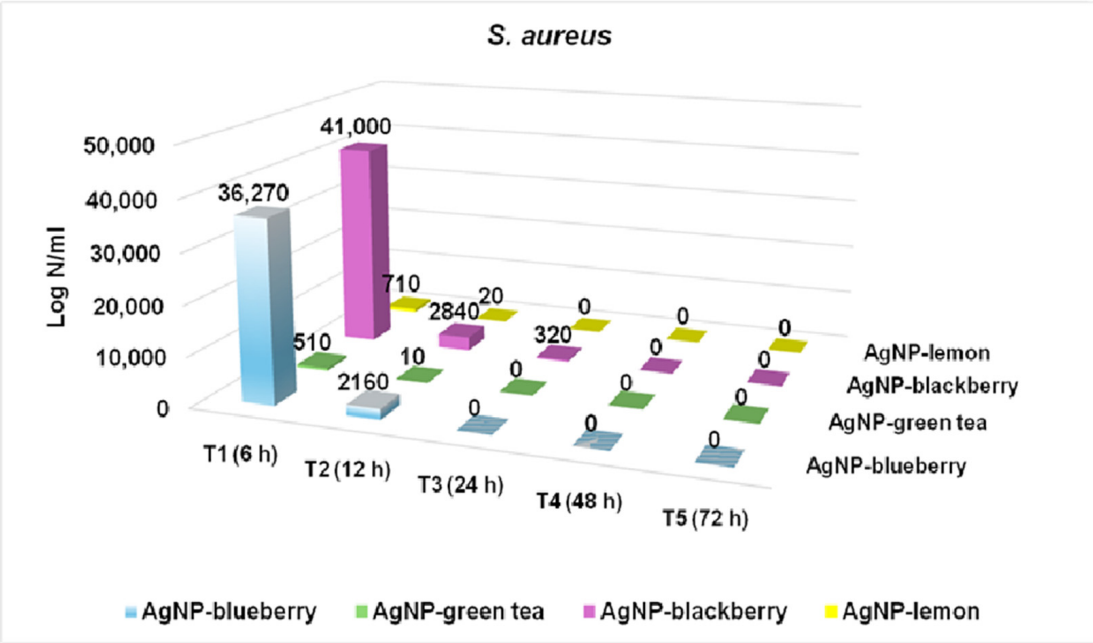

Figure 17. Results of applying the kill-time technique for *S. aureus*.

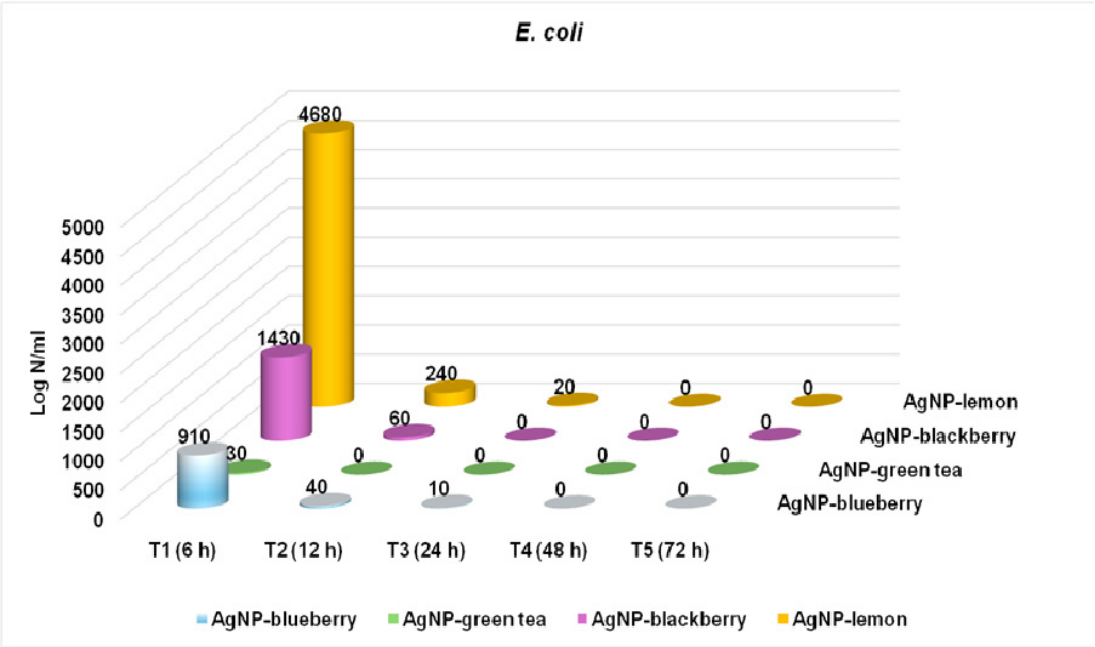

Figure 18. Results of applying the kill-time technique for *E. coli*.

4. Discussion

The results presented in the previous chapter describe the physico-chemical features and antimicrobial activities of silver nanoparticles synthesized with vegetal extracts.

Regarding the total polyphenol contents of these natural sources of antioxidants, according to Figure 1, we obtained 45 mg GAE/g for blueberries, 60 mg GAE/g for blackberries, approximately 20 mg GAE/g in lemon pulp, and 180 mg GAE/g in green tea dry leaves—all related to the dry substance mass. The antioxidant activity of an extract depends on a complex combination of factors, including the specific type of compounds, the synergy between them and the evaluation method. Blackberries contain(more than other berries, lemon pulp or tea leaves) not only polyphenols and flavones but also carotenoids,

sterols, terpenoids and vitamins A and C, with antioxidant activity, as shown recently in [57] and the interaction between different compounds in the extract can amplify the antioxidant effect, even if individually they are not the strongest. Thus, the antioxidant activity describing the capacity of the radicals scavenging, according to the DPPH assay, could be higher for AgNP–blackberry than for AgNP–blueberry and AgNP–lemon, being slightly higher than that of AgNP–green tea.

In the literature, we found the report of Li et al. [58], which describes blueberry varieties cultivated in China, and evidences a polyphenol content of about 161 mg GAE per 100 g of fresh substance, while Okan et al. [59] evidenced a polyphenol content of blueberries from Turkey as raging between 77 and 215 mg GAE per 100 g of fresh mass. Taking into account that water content represents about 90%, one could say that there is the same order of magnitude of polyphenols in 1 mg of GAE per 100 g fresh substance as in 1 mg per g of dry substance mass.

Castrejon et al. [60], like us, studied dried fruit samples and reported between 20 and 70 mg GAE per gram of dry matter for blueberry varieties from Korea—which matches rather well with our results.

Koczka et al. [61] found about 2000 mg GAE in blackberry fruits per 100 g of fresh matter, which would correspond to about 20 mg GAE per gram of dry matter—similar in order of magnitude to our results.

For lemon pulp samples, Gorinstein et al. [62] reported 154 ± 10.2 mg GAE per 100 g of fresh matter which corresponds to about 15 mg GAE/g of dry substance, while for the leaves of Chinese tea, Zhao et al. [63] found between 24.77 and 252.65 mg GAE per gram of dry matter, being also of the same order of magnitude as our results.

According to Figure 2, we found flavone contents of about 27 mg catechin per gram of dry matter in green tea, about 7.5 mg catechin/g in berries and around 2 mg catechin/g in lemon pulp.

In another article, Li et al. [58] presented the results of the analysis of 13 blueberry varieties with a flavone content between 161 and 512 mg per 100 g of fresh substance, which corresponds approximately to 16–51 mg of flavones per gram of dry matter being somehow higher than in our berries.

As given in Figure 3, the total antioxidant activity, expressed as the capacity of scavenging free radicals of DPPH, we found around 88% for green tea leaves and blackberry fruits, about 72% for blueberries and around 36% for lemon pulp. Xu et al. [64] studied fruits from different blueberry varieties in China and found values between 25 and 60% for the DPPH radical inhibition capacity, while Celant et al. [65] reported values of 53–74% in blackberry extracts, which is not far from our results. More recently, Vinci et al. [66] found a level of 95% in green tea extracts, and Garcia-Nicolas et al. [67] found 40% for lemon extract, which is comparable to the results of our investigation.

The spectral bands of silver nanoparticles that were recorded in the visible and near UV range, were characterized by maximum intensity positions at 425 nm for AgNP–lemon at 450 nm for AgNP–green tea, 458 nm for AgNP–blueberry and 429 nm for AgNP–blackberry (Figure 5). The same band shape and maximum position of 450 nm for silver nanoparticles synthesized with green tea extract was found by Demirel Bayik et al. [55]. Regarding the intensities of the spectral bands, in the case of AgNPs synthesized with berries, the time durations until stabilizing the suspensions were much longer than for lemon fruits or green tea; therefore, different processes could have occurred before the final spectra were recorded. It could be the degradation of some reductant molecules in the presence of oxygen and water and also of the catalytic silver and it could be the versatile equilibrium between silver ions and silver atoms in the reaction medium. This means that, in contact with the aqueous dispersion fluid, part of the silver atoms on the surface of the nanoparticles could

have been reoxidized and gradually released until some particles were depleted and for these reasons, the intensity of the final band could reach relatively lower values. As for the spectral band positions usually discussed in the literature, some authors have reported the maximum of the AgNP–lemon characteristic band at 441 nm after 15 days of reaction for different combinations of reactant proportions [68] or in the range 410–455 nm [41]. The spectral band with maximum absorption at 435 nm was recently reported by Hasan et al. [69], who accomplished the AgNP synthesis with green tea following a similar, but not identical, protocol (other concentrations and amounts of reactants).

Li et al. [49] used the same amounts of reactants but worked with Chinese blueberry leaves and reported the spectral maximum in the visible range at 434 nm wavelength. Ildiz et al. [70] reported the maximum of the characteristic spectral band of silver nanoparticles also synthesized with blueberry fruit extract in the wavelength range of 420–430 nm but using a slightly different protocol than the one applied in our study.

Kumar et al. [50], who utilized a double amount of silver salt against the same amount of blackberry extract as in our experiment, reported a 435 nm spectral band that stabilized after 14 days and with about double the intensity for light absorption, as expected.

Starting from the same amount of silver nitrate for all samples described by us, the AgNP–green tea suspension presented the spectral band with the highest intensity—about twice compared to AgNP–lemon, which denotes a better capacity of converting silver ions into silver nanoparticles.

Thus, it seems that the use of green tea offers the most efficient synthesis, evidenced by the highest intensity spectral band and the shortest stabilization time, with respect to the best reduction of ionic silver. The comparison with the previously published research reports, mentioned in the frame of this discussion, shows rather concordant results regarding the position of the characteristic spectral band of nanosized silver. Basically, the wavelength of the maximum absorption is related to the size of the particles most frequent in the sample as well as to the electro-optical properties of the surrounding medium of the metal cores. The cited authors did not offer the characterization of the antioxidant properties of the vegetal materials used for nanoparticle synthesis. For complex and different compositions of the vegetal extracts, when provided by various sources, it is unavoidable that the organic shell coating of the silver particles is different, with similar but not identical reduction capacity, with similar but not the same electro-optical features.

These SEM investigation results revealed that silver nanoparticles have the most frequent diameters between 25 and 65 nm (Figure 6a–d) with the tendency of neighbor particle association in small clusters. The results obtained for AgNP–green tea evidencing 30–60 nm particles are in agreement with the TEM data of 42 $\pm$ 17 nm, reported by Demirel Bayik et al. [55] for the same initial concentration of 1 mM of silver nitrate.

The dark field microscopy analysis showed 15–55 nm size of silver nanoparticles prepared with lemon and green tea and 22–70 nm diameters for AgNP synthesized with berries (Figure 7). The silver nanoparticles are visible in optical microscopy due to the plasmonic emission specific to nanostructured objects made of noble metals, like silver and gold, the light emission covering a volume two orders of magnitude larger than that of the metal nanocores.

Although, in the available literature, we did not find size measurements carried out in dark-field optical microscopy for this kind of silver nanoparticles; however, there are dimensional descriptions based on electron microscopy. Thus, using transmission electron microscopy, Prathna et al. [68] measured the diameters of silver nanoparticles synthesized with lemon extract and reported between 25 and 50 nm values while Li et al. [49] reported 10 to 30 nm sizes for AgNPs synthesized with blueberry extract, and Kumar et al. [50] found particle diameter values between 12 and 50 nm for AgNPs synthesized with blackberry

extract. As well, using scanning electron microscopy, Hasan et al. [69] evidenced that AgNPs synthesized with green tea were characterized by 35 to 50 nm diameters.

We might say that our results are in good agreement with the existing literature for similar products from the viewpoint of granularity with the mention that electron microscopy data evidenced precisely the metal cores while dark field microscopy estimates the particle size from that of the resonant plasmonic emissions.

The crystallinity features of the AgNP prepared with vegetal extracts were evidenced by X-ray diffractometry (Figure 8a–d) the specific maxima angles being given in Table 1.

The intensity of the X-ray diffraction peaks mainly denotes the concentration of crystallized material but also depends on various other factors [71], which can cause increases or decreases in intensity compared to the theoretically hypothesized one. One of these is the phenomenon of so-called X-ray fluorescence, occurring right inside the crystal which is explained by the successive diffraction/scattering of already diffracted X-rays, thus extinct within the crystal and, as a result, the intensity of the radiation beam detected outside the sample decreases. It occurs preferentially due to the presence of metal atoms as impurities in the metal of the X-ray emitting cathode—in the case of the copper cathode of the Shimadzu Lab 6000 device these being unavoidably cobalt, manganese and iron. But the AgNP–green tea sample also contains both manganese and cobalt and Iron according to the literature [72], which can be correlated with the lower relative intensity of the corresponding diffraction maxima compared to the other AgNP samples. Also, in commercial lemon fruits manganese was found [73], as well as cobalt [74], and iron [75]). In contrast, blueberry fruits do not present any of these elements [76], though various oligoelements and heavy metals were precisely found there. So we can assume that compared to AgNP synthesized with blueberries, the lower relative intensity of the diffraction maxima in AgNP–green tea, AgNP–lemon and AgNP–blackberry is likely to be correlated with the decrease in the flux of X-rays diffracted on silver crystals but still sequentially diffracted in the sample on heavy metal atoms of manganese, iron, and cobalt from the fruit extracts.

The diffraction maxima of silver nanoparticles synthesized with lemon extract were reported by Khane et al. [45] at angles of 38.18°, 44.34°, 64.53°, and 77.46°, in good agreement with the standards and our reported results. Studying silver particles synthesized with blackberry extract, Kumar et al. [50] found similar diffraction angle values of 38.04°, 44.06°, 64.34° and 77.17. Analyzing AgNP particles with blueberry extract, Li et al. [49] identified the characteristic diffraction peaks of crystallized silver at 38.2°, 44.4°, 64.5°, and 77.5°.

For silver nanoparticles synthesized with green tea, Safa &Koohestani [77] revealed the diffraction peaks at angles of 38.1°, 44.4°, 64.5°, and 77.0°. Compared with all these reports, the values obtained by us are in rather good agreement.

The hydrodynamic diameters and Zeta potential values were determined by dynamic light scattering, as presented in Figures 9–13.

As known, the DLS method allow sfor estimating the hydrodynamic diameter of colloidal particles in Brownian motion within the dispersion fluid, which depends not only on the size of the metal cores and of the molecular shell but also includes adjacent fluid layers in the immediate vicinity, so that, in many cases, the values of this diameter, D_h, are larger than those of the nanoparticle sizes measured by other microstructural techniques. On another side, the dark field microscopy method estimates the size of metal colloidal nanoparticles deposited on a microscope slide which is possible due to the plasmon resonant emission—bearing information only on the source-emitter metal particles and also on the electro-optical properties of the molecular shell around the metal cores. One could say shortly that the D_h is usually the largest because it includes waters of hydration [78].

The Zeta potential values for AgNP–lemon and AgNP–green tea are rather low negative values (−2.8 mV and 4.3 mV) raising the issue of the suspension stability. Other authors found a small positive Zeta potential between +7 mV and +13 mV for AgNP synthesized with bee bread extracts [79]. We assumed that the remarkable stability of these samples, which did not precipitate for months when kept in the refrigerator, was ensured less by electrostatic repulsion, but dominantly by the steric repulsion forces corresponding to the possible thicker shell of organic matter, which also increases the hydrodynamic diameter compared to that emphasized by microscope measurement.

Zeta potential is known to be generated by the electrical charges on the surface of the nanoparticles suspended in a fluid medium. The electrical repulsion between particles with an electrical charge of the same sign can ensure the stability of the suspension by preventing the aggregation of neighboring particles. A molecular shell more consistent although with less electrical charge can also act in the same way, covering the particles with a thicker layer of substance, thus preventing them from approaching and merging—steric repulsion. This way we can describe the different behavior of AgNP suspensions synthesized with berries, on one side, where the Zeta potential has higher values than for the AgNP–lemon and AgNP–green tea suspensions, on the other side, where the Zeta potential values are the lowest. The moderate electrical charge of the AgNP suspensions synthesized with berries is probably due to organic ions such as ascorbate or citrate—ascorbic acid as well as citric acid being present in significant concentration in berries [80,81]—thus electric stability being dominant. In the case of AgNP–lemon and AgNP–green tea, the organic shell may be more complex, with the retention on the surface of the metal cores also of larger molecular components with lower net electric charge but ensuring a greater spatial distance—steric repulsion being the dominant one. The higher values of D_h—double for AgNP–lemon and AgNP–green tea compared to the berry case, support this assumption. We also emphasize that it would be possible that, initially, the AgNP samples synthesized with berries also presented a consistent coating of ions but large molecules too; however, it is noticeable the completion of the AgNP suspensions synthesized with berries took several days (14 and 27 days, respectively). During this time, the Brownian motions of colloidal particles in fluid dispersion could have led to the loss of large molecules from the shell—more loosely attached, i.e., through weaker van der Waals forces than molecular ions capable of stronger electrical interactions.

Khane et al. [45] synthesized silver nanoparticles with lemon extract, reporting a hydrodynamic diameter D_h of 82.5 nm, with a polydispersity index of 0.248, while Prathna et al. [68] found a value similar to our D_h, of about 120 nm, i.e., the hydrodynamic diameter of 153.68 nm with a PDI of 0.206, since, most probably in each case, the composition of the antioxidants in the used lemons were different as well as of the other organic molecules and thus, the metal core coating layers have different thicknesses and properties. Also, a large hydrodynamic diameter of 124 nm was reported for AgNPs obtained using fungal synthesis by Raut et al. [82].

Prathna et al. [66] and Khane et al. [45] evidenced negative Zeta potentials, for example, −29 mV or −27 mV, which were explained based on the negative charge of their silver nanoparticles synthesized with lemon extract, given by citrate ions in significant concentration around the metal cores.

Zuorro et al. [81] also succeeded in preparing silver nanoparticles using blueberry extract for the silver reduction, with the hydrodynamic diameter ranging between 25 and 65 nm and the Zeta potential ranging between –35.6 and –20.5 mV. Other authors reported a hydrodynamic diameter about twice as large as for the sample studied by us of 146.3 nm [50] and a polydispersity index also about twice as large as the values found by us (PDI = 0.27) for the synthesis of AgNP–blackberries.

All these results regarding the four AgNP suspensions revealed fine granularity and good stability over time, which recommends them for biomedical applications. Studying the antimicrobial activity of the four AgNP samples synthesized by us with vegetal extracts, we first measured the diameters of the germ growth inhibition with the agar diffusion method. For *S. aureus*, the diameter values ranged between 7 and 15 mm, while for *E. coli* we found they were between 11 and 18 mm. Thus, the higher susceptibility of *E. coli* compared to *S. aureus* to the action of the antimicrobial silver nanoparticle suspensions was illustrated.

We noticed the largest growth inhibition zones for AgNP–green tea against *S. aureus*, while against *E. coli*, the samples of AgNP–lemon and AgNP–blackberry were proved to be the most efficient.

The direct relationship between the absorption band intensity, i.e., the nanoparticle concentration and the antimicrobial effect was evidenced for *S. aureus* but not *for E. coli. S. aureus* treated with silver nanoparticle suspensions gave higher diameters of the growth inhibition for AgNP–green tea and AgNP–blueberry and smaller diameters for AgNP–blackberry and AgNP–lemon (Figure 15) with respect to the order of the absorption band intensities (Figure 5). *E. coli* growth, however, was more affected by AgNP–lemon and AgNP–blackberry; thus, the susceptibility of this germ to other antimicrobial agents should be considered. Certain silver ions could be present but only at dynamic equilibrium with silver atoms released from the nanoparticle surface as long as the absorption band intensities remained the same over couple of months. The attention could be focused on the fruit extracts that, possibly, were not entirely needed for the reduction reactions. In the case of lemon, the high content of vitamin C—higher than in other fruits or in green tea leaves—seems to be of actual interestas its antimicrobial action is already recognized. Some authors [83,84] have shown that vitamin C has significant antimicrobial activity against Gram-negative germs—like *E. coli*, in our case.

The susceptibility of *E. coli* to the vitamin C antimicrobial effect could explain the large inhibition zones for AgNP–lemon suspension (18.5 mm in Figure 15).

As for the high effect of the AgNP–blackberry sample (also 18.5 mm in Figure 15), we believe that blackberry extract itself, also only partially consumed for the silver reduction reactions has supplemented the antimicrobial effect of silver nanoparticles on *E. coli*. The literature reports support this hypothesis. Indeed, it was found that blackberry extract exhibits antimicrobial activity against *E. coli* and coliform bacteria, according to [85,86].

The remarkable efficacy of AgNP synthesized with green tea was reported also by Raza et al. [87], who demonstrated that such nanoparticles destroy Gram-negative pathogens, like *E. coli*, by 80% compared to 40% in the case of ampicillin administered at the same concentration.

Khane et al. [45] worked with lemon peel extract to obtain silver nanoparticles and evidenced their efficacy also using the diffusimetric method; the diameters of the microbial growth inhibition zones were 14 mm for *S. aureus* and 20 mm for *E. coli*. By comparison, we obtained 7.5 mm for *S. aureus*, and 18.6 mm for *E. coli*, which represents a fairly significant antimicrobial efficiency considering that we used lemon juice, which is less concentrated in polyphenols and flavones than the peel. Demirbas et al. [46] prepared AgNP particles synthesized with blackberry extract evidencing growth inhibition areas with a diameter of 11 mm for *E. coli* and 16 mm for *S. aureus*—data with which our results are not in good agreement, possibly because some different substances with antioxidant or antimicrobial effects are contained in the blackberry fruits from different sources.

Searching the available literature for studies focused on silver nanoparticles synthesized with vegetal extracts and tested with kill-time assay, we found Loo et al. [88], who applied this method for testing the antimicrobial activity of AgNP obtained with Indian

tea extract and demonstrated its efficiency against several species of Gram-negative germs, including *E. coli*. The killing time was about 1–2h against Gram-negative germs.

Studying the cytotoxicity of silver ions has led to the proposal of several hypotheses regarding their interaction mechanisms with living cells—hypotheses that can also be taken up in the case of silver nanoparticles, vectors of silver ions that can be released by reoxidizing the atoms on their surface.

Ag^+ ions first encounter the cell wall, which covers the bacterial cell membrane, protecting it. This is mainly formed by peptidoglycans and the positively charged silver ions can form molecular complexes with some electron donor groups (with a partial negative charge, due to oxygen or nitrogen) in the peptidoglycan molecules, influencing the permeability properties of the cell envelope, so they can next reach the cell membrane—the plasmalemma.

Ag^+ ions can also penetrate the cell membrane, interacting with cell organelles and influencing metabolic processes in the cytoplasm [89], an important role being attributed to the generation of reactive oxygen species (ROS) and the interaction with proteins and DNA molecules.

The anomalies generated by the impact of AgNPs with the cell membrane are assumed to be in the form of small, microscopic pits [90] resulting from the destructuring and fragmentation of the membrane surface [91], as demonstrated experimentally after the administration of submillimolar concentrations of AgNPs in various cultures of microorganisms, and studying the images obtained by special transmission electron microscopy techniques.

Such membrane damage can dramatically disrupt its functions, especially permeability as well as cell viability [92]. In some microbial species, the effects of AgNP particles can be stronger than those of Ag^+ ions as demonstrated by Kim et al. [93] for *E. coli* and *S. aureus*.

The toxicity induced by the production of high levels of reactive oxygen species (ROS)—such as hydroxyl radicals (OH), ionized molecular oxygen (O_2^-), hydrogen peroxide (H_2O_2), etc.—is due to their oxidizing effect, which mainly affects lipids in the membrane structures of the plasmalemma and in the membranes of cellular organelles, for example, mitochondria—the seat of vital cellular respiration processes.

Thus, membranes with peroxidized lipids become destabilized and lose their permeability functions for ions (sodium, potassium, calcium, etc.), which compromises communication with the environment. As a result, cells suffer irreparable alterations of vital processes and die.

5. Conclusions

Silver nanoparticles synthesized with natural reducers from plant extracts presented physico-chemical characteristics comparable to those reported in the literature, proving them to be suitable for biomedical applications.

The antimicrobial activity of colloidal silver suspensions was evidenced both for Gram-positive bacteria, represented here by *S. aureus* and for Gram-negative bacteria, with different sensitivities to pharmaceutical agents (represented by *E. coli*).

The application of the diffusimetric method highlighted the largest inhibition zones of 18 mm for *E. coli* treated with AgNP–blackberry and AgNP–lemon, while 15 mm size inhibition zones resulted for *S. aureus* treated with AgNP–green tea.

The application of the kill-time technique allowed us to highlight the fact that for *S. aureus*, the AgNP–green tea and AgNP–lemon samples led to the best results. For *E. coli*, the AgNP–green tea particles were the most effective. Thus, the AgNP–green tea sample proved to be the most effective for both Gram-positive and Gram-negative bacteria—using both the applied techniques.

For green tea, the highest content of polyphenols, the highest content of flavones and the highest total antioxidant capacity were found.

Author Contributions: Conceptualization: D.C. and R.P.; methodology, R.P., C.R., L.O., D.H., D.L., I.M., D.C. and M.-N.G.; investigation, R.P., C.R., D.H., D.L., I.M., D.C. and M.-N.G.; writing—original draft preparation, D.C. and R.P.; writing—review and editing, R.P., C.R., L.O., D.H., D.L., D.C. and M.-N.G.; visualization, D.C.; supervision, L.O., D.C. and M.-N.G. All authors have read and agreed to the published version of the manuscript.

Funding: This research received no external funding.

Institutional Review Board Statement: Not applicable.

Informed Consent Statement: Not applicable.

Data Availability Statement: The data presented in this study are available on request from the corresponding author.

Conflicts of Interest: The authors declare no conflicts of interest.

References

1. Yaqoob, A.A.; Umar, K.; Ibrahim, M.N.M. Silver nanoparticles: Various methods of synthesis, size affecting factors and their potential applications—A review. *Appl. Nanosci.* **2020**, *10*, 1369–1378. [CrossRef]
2. Prasad, R.; Deena, S.; Rajesh, C.; Pandit, V.K.; Pathan, H.M. Employing green synthesized silver nanoparticles as light harvesters in nanostructured solar cells. *J. Renew. Sustain. Energy* **2013**, *5*, 031615. [CrossRef]
3. Kalfagiannis, N.; Karagiannidis, P.G.; Pitsalidis, C.; Panagiotopoulos, N.T.; Gravalidis, C.; Kassavetis, S.; Patsalas, P.; Logothetidis, S. Plasmonic silver nanoparticles for improved organic solar cells. *Sol. Energy Mater. Sol. Cells* **2012**, *104*, 165–174. [CrossRef]
4. Walshe, J.; Carron, P.M.; McLoughlin, C.; McCormack, S.; Doran, J.; Amarandei, G. Nanofluid development using silver nanoparticles and organic-luminescent molecules for solar-thermal and hybrid photovoltaic-thermal applications. *Nanomaterials* **2020**, *10*, 1201. [CrossRef]
5. Khan, S.A.; Jain, M.; Pandey, A.; Pant, K.K.; Ziora, Z.M.; Blaskovich, M.A.; Aminabhavi, T.M. Leveraging the potential of silver nanoparticles-based materials towards sustainable water treatment. *J. Environ. Manag.* **2022**, *319*, 115675. [CrossRef]
6. Rostami-Vartooni, A.; Nasrollahzadeh, M.; Alizadeh, M. Green synthesis of seashell supported silver nanoparticles using Bunium persicum seeds extract: Application of the particles for catalytic reduction of organic dyes. *J. Colloid Interface Sci.* **2016**, *470*, 268–275. [CrossRef]
7. Atarod, M.; Nasrollahzadeh, M.; Sajadi, S.M. Euphorbia heterophylla leaf extract mediated green synthesis of Ag/TiO_2 nanocomposite and investigation of its excellent catalytic activity for reduction of variety of dyes in water. *J. Colloid Interface Sci.* **2016**, *452*, 272–279. [CrossRef]
8. Zahran, M.; Khalifa, Z.; Zahran, M.A.H.; Azzem, M.A. Recent advances in silver nanoparticle-based electrochemical sensors for determining organic pollutants in water: A review. *Mater. Adv.* **2021**, *2*, 7350–7365. [CrossRef]
9. Abbas, A.; Amin, H.M. Silver nanoparticles modified electrodes for electroanalysis: An updated review and a perspective. *Microchem. J.* **2022**, *175*, 107166. [CrossRef]
10. Ivanišević, I. The role of silver nanoparticles in electrochemical sensors for aquatic environmental analysis. *Sensors* **2023**, *23*, 3692. [CrossRef]
11. Roy, B.; Bairi, P.; Nandi, A.K. Selective colorimetric sensing of mercury(ii) using turn off–turn on mechanism from riboflavin stabilized silver nanoparticles in aqueous medium. *Analyst* **2011**, *136*, 3605. [CrossRef] [PubMed]
12. Fernández-Lodeiro, J.; Núñez, C.; Oliveira, E.; Capelo, J.L.; Lodeiro, C. 1D chain fluorescein-functionalized gold and silver nanoparticles as new optical mercury chemosensor in aqueous media. *J. Nanopart. Res.* **2013**, *15*, 1828. [CrossRef]
13. Lee, D.K.; Kang, Y.S. Synthesis of silver nanocrystallites by a new thermal decomposition method and their characterization. *ETRI J.* **2004**, *26*, 252–256. [CrossRef]
14. Boutinguiza, M.; Comesaña, R.; Lusquiños, F.; Riveiro, A.; Del Val, J.; Pou, J. Production of silver nanoparticles by laser ablation in open air. *Appl. Surf. Sci.* **2015**, *336*, 108–111. [CrossRef]
15. Tsuji, T.; Iryo, K.; Watanabe, N.; Tsuji, M. Preparation of silver nanoparticles by laser ablation in solution: Influence of laser wavelength on particle size. *Appl. Surf. Sci.* **2002**, *202*, 80–85. [CrossRef]
16. Mavani, K.; Shah, M. Synthesis of silver nanoparticles by using sodium borohydride as a reducing agent. *Int. J. Eng. Res. Technol.* **2013**, *2*, 1–5.

17. Dasaradhudu, Y.; Srinivasan, M.A. Synthesis and characterization of silver nano particles using co-precipitation method. *Mater. Today Proc.* **2020**, *33*, 720–723. [CrossRef]
18. Ivask, A.; Kurvet, I.; Kasemets, K.; Blinova, I.; Aruoja, V.; Suppi, S.; Vija, H.; Käkinen, A.; Titma, T.; Heinlaan, M.; et al. Size-dependent toxicity of silver nanoparticles to bacteria, yeast, algae, crustaceans and mammalian cells in vitro. *PLoS ONE* **2014**, *9*, e102108. [CrossRef]
19. Singh, R.; Shedbalkar, U.U.; Wadhwani, S.A.; Chopade, B.A. Bacteriagenic silver nanoparticles: Synthesis, mechanism, and applications. *Appl. Microbiol. Biotechnol.* **2015**, *99*, 4579–4593. [CrossRef]
20. Al-Asbahi, M.G.; Al-Ofiry, B.A.; Saad, F.A.; Alnehia, A.; Al-Gunaid, M.Q. Silver nanoparticles biosynthesis using mixture of *Lactobacillus sp.* and *Bacillus sp.* growth and their antibacterial activity. *Sci. Rep.* **2024**, *14*, 10224. [CrossRef]
21. Alsamhary, K.I. Eco-friendly synthesis of silver nanoparticles by *Bacillus subtilis* and their antibacterial activity. *Saudi J. Biol. Sci.* **2020**, *27*, 2185–2191. [CrossRef]
22. Yassin, M.A.; Elgorban, A.M.; El-Samawaty, A.E.R.M.; Almunqedhi, B.M. Biosynthesis of silver nanoparticles using *Penicillium verrucosum* and analysis of their antifungal activity. *Saudi J. Biol. Sci.* **2021**, *28*, 2123–2127. [CrossRef] [PubMed]
23. Guilger-Casagrande, M.; Lima, R.D. Synthesis of silver nanoparticles mediated by fungi: A review. *Front. Bioeng. Biotechnol.* **2019**, *7*, 287. [CrossRef] [PubMed]
24. Wang, D.; Xue, B.; Wang, L.; Zhang, Y.; Liu, L.; Zhou, Y. Fungus-mediated green synthesis of nano-silver using *Aspergillus sydowii* and its antifungal/antiproliferative activities. *Sci. Rep.* **2021**, *11*, 10356. [CrossRef] [PubMed]
25. Song, J.Y.; Kim, B.S. Rapid biological synthesis of silver nanoparticles using plant leaf extracts. *Bioprocess Biosyst. Eng.* **2009**, *32*, 79–84. [CrossRef]
26. Logeswari, P.; Silambarasan, S.; Abraham, J. Synthesis of silver nanoparticles using plant extracts and analysis of their antimicrobial property. *J. Saudi Chem. Soc.* **2015**, *19*, 311–317. [CrossRef]
27. Ahmed, S.; Ahmad, M.; Swami, B.L.; Ikram, S. Green synthesis of silver nanoparticles using *Azadirachta indica* aqueous leaf extract. *J. Rad. Res. Appl. Sci.* **2016**, *9*, 1–7. [CrossRef]
28. Vanlalveni, C.; Lallianrawna, S.; Biswas, A.; Selvaraj, M.; Changmai, B.; Rokhum, S.L. Green synthesis of silver nanoparticles using plant extracts and their antimicrobial activities: A review of recent literature. *RSC Adv.* **2021**, *11*, 2804–2837. [CrossRef]
29. Abada, E.; Mashraqi, A.; Modafer, Y.; Al Abboud, M.A.; El-Shabasy, A. Review green synthesis of silver nanoparticles by using plant extracts and their antimicrobial activity. *Saudi J. Biol. Sci.* **2024**, *31*, 103877. [CrossRef]
30. Goswami, S.R.; Sahareen, T.; Singh, M.; Kumar, S. Role of biogenic silver nanoparticles in disruption of cell–cell adhesion in *Staphylococcus aureus* and *Escherichia coli* biofilm. *J. Ind. Eng. Chem. Res.* **2015**, *26*, 73–80. [CrossRef]
31. Ali, S.G.; Jalal, M.; Ahmad, H.; Sharma, D.; Ahmad, A.; Umar, K.; Khan, H.M. Green synthesis of silver nanoparticles from *Camellia sinensis* and its antimicrobial and antibiofilm effect against clinical isolates. *Materials* **2022**, *15*, 6978. [CrossRef] [PubMed]
32. Widatalla, H.A.; Yassin, L.F.; Alrasheid, A.A.; Ahmed, S.A.R.; Widdatallah, M.O.; Eltilib, S.H.; Mohamed, A.A. Green synthesis of silver nanoparticles using green tea leaf extract, characterization and evaluation of antimicrobial activity. *Nanoscale Adv.* **2022**, *4*, 911–915. [CrossRef]
33. Wirwis, A.; Sadowski, Z. Green synthesis of silver nanoparticles: Optimizing green tea leaf extraction for enhanced physicochemical properties. *ACS Omega* **2023**, *8*, 30532–30549. [CrossRef]
34. Kahrilas, G.A.; Wally, L.M.; Fredrick, S.J.; Hiskey, M.; Prieto, A.L.; Owens, J.E. Microwave-assisted green synthesis of silver nanoparticles using orange peel extract. *ACS Sustain. Chem. Eng.* **2014**, *2*, 367–376. [CrossRef]
35. Alkhulaifi, M.M.; Alshehri, J.H.; Alwehaibi, M.A.; Awad, M.A.; Al-Enazi, N.M.; Aldosari, N.S.; Ashraf, A. Green synthesis of silver nanoparticles using *Citrus limon* peels and evaluation of their antibacterial and cytotoxic properties. *Saudi J. Biol. Sci.* **2020**, *27*, 3434–3441. [CrossRef]
36. Mickky, B.; Elsaka, H.; Abbas, M.; Gebreil, A.; Shams Eldeen, R. Orange peel-mediated synthesis of silver nanoparticles with antioxidant and antitumor activities. *BMC Biotechnol.* **2024**, *24*, 66. [CrossRef]
37. Kalia, A.; Manchanda, P.; Bhardwaj, S.; Singh, G. Biosynthesized silver nanoparticles from aqueous extracts of sweet lime fruit and callus tissues possess variable antioxidant and antimicrobial potentials. *Inorg. Nano-Met. Chem.* **2020**, *50*, 1053–1062. [CrossRef]
38. Kumar, D.; Sharma, N. Green chemistry approach: Synthesis of silver nanoparticles by using lime juice (*Citrus aurantifolia*) extract and their evaluation as antibacterial agent. *J. Indian Chem. Soc.* **2014**, *91*, 1667–1674.
39. Abdelrazik, M.; Elkotaby, H.H.; Yousef, A.; El-Sayed, A.F.; Khedr, M. Green synthesis of silver nanoparticles derived from lemon and pomegranate peel extracts to combat multidrug-resistant bacterial isolates. *J. Genet. Eng. Biotechnol.* **2023**, *21*, 97. [CrossRef]
40. Rizwana, H.; Alwhibi, M.S.; Al-Judaie, R.A.; Aldehaish, H.A.; Alsaggabi, N.S. Sunlight-mediated green synthesis of silver nanoparticles using the berries of *Ribes rubrum* (red currants): Characterisation and evaluation of their antifungal and antibacterial activities. *Molecules* **2022**, *27*, 2186. [CrossRef]
41. Umoren, S.A.; Nzila, A.M.; Sankaran, S.; Solomon, M.M.; Umoren, P.S. Green synthesis, characterization and antibacterial activities of silver nanoparticles from strawberry fruit extract. *Pol. J. Chem. Technol.* **2017**, *19*, 128–136. [CrossRef]

42. Stevanović, M.S.; Zvezdanović, J.B.; Stanojević, L.P.; Stanojević, J.S.; Petrović, S.M.; Cakić, M.D.; Cvetković, D.J. Synthesis, characterization and antioxidant activity of silver nanoparticles stabilized by aqueous extracts of wild blackberry (*Rubus* spp.) and raspberry (*Rubus idaeus* L.) leaves. *Adv. Technol.* **2019**, *8*, 47–58. [CrossRef]
43. Nadagouda, M.N.; Iyanna, N.; Lalley, J.; Han, C.; Dionysiou, D.D.; Varma, R.S. Synthesis of silver and gold nanoparticles using antioxidants from blackberry, blueberry, pomegranate, and turmeric extracts. *ACS Sustain. Chem. Eng.* **2014**, *2*, 1717–1723. [CrossRef]
44. Niluxsshun, M.C.D.; Masilamani, K.; Mathiventhan, U. Green synthesis of silver nanoparticles from the extracts of fruit peel of *Citrus tangerina*, *Citrus sinensis*, and *Citrus limon* for antibacterial activities. *Bioinorg. Chem. Appl.* **2021**, *2021*, 6695734. [CrossRef] [PubMed]
45. Khane, Y.; Benouis, K.; Albukhaty, S.; Sulaiman, G.M.; Abomughaid, M.M.; Al Ali, A.; Dizge, N. Green synthesis of silver nanoparticles using aqueous *Citrus limon* zest extract: Characterization and evaluation of their antioxidant and antimicrobial properties. *Nanomaterials* **2022**, *12*, 2013. [CrossRef]
46. Demirbas, A.; Yilmaz, V.; Ildiz, N.; Baldemir, A.; Ocsoy, I. Anthocyanins-rich berry extracts directed formation of Ag NPs with the investigation of their antioxidant and antimicrobial activities. *J. Mol. Liq.* **2017**, *248*, 1044–1049. [CrossRef]
47. Dhulappanavar, G.; Hungund, B.; Ayachit, N.; Bhakat, A.; Singh, P.P.; Priya, S.; Pawar, J.; Vinchurkar, P.; Henry, R. Characterization of silver nanoparticles biosynthesized using lemon juice. In Proceedings of the International Conference on Nanoscience, Engineering and Technology (ICONSET 2011), Chennai, India, 28–30 November 2011; pp. 258–262.
48. Nakhjavani, M.; Nikkhah, V.; Sarafraz, M.M.; Shoja, S.; Sarafraz, M. Green synthesis of silver nanoparticles using green tea leaves: Experimental study on the morphological, rheological and antibacterial behaviour. *Heat and Mass Transf.* **2017**, *53*, 3201–3209. [CrossRef]
49. Li, K.; Ma, C.; Jian, T.; Sun, H.; Wang, L.; Xu, H.; Cheng, X. Making good use of the byproducts of cultivation: Green synthesis and antibacterial effects of silver nanoparticles using the leaf extract of blueberry. *J. Food Sci. Technol.* **2017**, *54*, 3569–3576. [CrossRef]
50. Kumar, B.; Smita, K.; Cumbal, L.; Debut, A. Green synthesis of silver nanoparticles using Andean blackberry fruit extract. *Saudi J. Biol. Sci.* **2017**, *24*, 45–50. [CrossRef]
51. Singleton, V.L.; Orthofer, R.; Lamuela-Raventós, R.M. Analysis of total phenols and other oxidation substrates and antioxidants by means of Folin-Ciocalteu reagent. In *Methods in Enzymology*, 1st ed.; Packer, L., Ed.; Elsevier: Cambridge, MA, USA, 1999; Volume 299, pp. 152–178.
52. Dewanto, V.; Wu, X.; Adom, K.K.; Liu, R.H. Thermal processing enhances the nutritional value of tomatoes by increasing total antioxidant activity. *J. Agric. Food Chem.* **2002**, *50*, 3010–3014. [CrossRef]
53. Molyneux, P. The use of the stable free radical diphenylpicrylhydrazyl (DPPH) for estimating antioxidant activity. *Songklanakarin J. Sci. Technol.* **2004**, *26*, 211–219.
54. Bonev, B.; Hooper, J.; Parisot, J. Principles of assessing bacterial susceptibility to antibiotics using the agar diffusion method. *J. Antimicrob. Chemother* **2008**, *61*, 1295–1301. [CrossRef] [PubMed]
55. Demirel Bayik, G.; Baykal, B. Impact of Plant Species on the Synthesis and Characterization of Biogenic Silver Nanoparticles: A Comparative Study of *Brassica oleracea*, *Corylus avellana*, and *Camellia sinensis*. *Nanomaterials* **2024**, *14*, 1954. [CrossRef] [PubMed]
56. Lima, B.G.A.; Silva, R.R.; Meira, H.M.; Durval, I.J.B.; Macedo Bezerra Filho, C.; Silva, T.A.L.; Sarubbo, L.A.; Luna, J.M. Synthesis and Characterization of Silver Nanoparticles Stabilized with Biosurfactant and Application as an Antimicrobial Agent. *Microorganisms* **2024**, *12*, 1849. [CrossRef]
57. Gil-Martínez, L.; Mut-Salud, N.; Ruiz-García, J.A.; Falcón-Piñeiro, A.; Maijó-Ferré, M.; Baños, A.; Gómez-Caravaca, A.M. Phytochemicals determination, and antioxidant, antimicrobial, anti-inflammatory and anticancer activities of blackberry fruits. *Foods* **2023**, *12*, 1505. [CrossRef]
58. Li, D.; Li, B.; Ma, Y.; Sun, X.; Lin, Y.; Meng, X. Polyphenols, anthocyanins, and flavonoids contents and the antioxidant capacity of various cultivars of highbush and half-high blueberries. *J. Food Compos. Anal.* **2017**, *62*, 84–93. [CrossRef]
59. Okan, O.T.; Deniz, I.; Yayli, N.; Sat, I.G.; Oz, M.; Hatipoglu Serdar, G. Antioxidant activity, sugar content and phenolic profiling of blueberries cultivars: A comprehensive comparison. *Not. Bot. Horti. Agrobo. Cluj-Napoca* **2018**, *46*, 639–652. [CrossRef]
60. Castrejon, A.D.R.; Eichholz, I.; Rohn, S.; Kroh, L.W.; Huyskens-Keil, S. Phenolic profile and antioxidant activity of highbush blueberry (*Vaccinium corymbosum* L.) during fruit maturation and ripening. *Food Chem.* **2008**, *109*, 564–572. [CrossRef]
61. Koczka, N.; Stefanovits-Banyai, E.; Prokaj, E. Element composition, total phenolics and antioxidant activity of wild and cultivated blackberry (*Rubus fruticosus* L.) fruits and leaves during the harvest time. *Not. Bot. Horti. Agrobo. Cluj-Napoca* **2018**, *46*, 563–569. [CrossRef]
62. Gorinstein, S.; Martín-Belloso, O.; Park, Y.S.; Haruenkit, R.; Lojek, A.; Číž, M.; Trakhtenberg, S. Comparison of some biochemical characteristics of different citrus fruits. *Food Chem.* **2001**, *74*, 309–315. [CrossRef]
63. Zhao, C.N.; Tang, G.Y.; Cao, S.Y.; Xu, X.Y.; Gan, R.Y.; Liu, Q.; Mao, Q.Q.; Shang, A.; Li, H.B. Phenolic profiles and antioxidant activities of 30 tea infusions from green, black, oolong, white, yellow, and dark teas. *Antioxidants* **2019**, *8*, 215. [CrossRef] [PubMed]

64. Xu, G.; Liu, D.; Chen, J.; Ye, X.; Ma, Y.; Shi, J. Juice components and antioxidant capacity of citrus varieties cultivated in China. *Food Chem.* **2008**, *106*, 545–551. [CrossRef]
65. Celant, V.M.; Braga, G.C.; Vorpagel, J.A.; Salibe, A.B. Phenolic composition and antioxidant capacity of aqueous and ethanolic extracts of blackberries. *Rev. Bras. Frutic.* **2016**, *38*, e-411. [CrossRef]
66. Vinci, G.; D'Ascenzo, F.; Maddaloni, L.; Prencipe, S.A.; Tiradritti, M. The influence of green and black tea infusion parameters on total polyphenol content and antioxidant activity by ABTS and DPPH assays. *Beverages* **2022**, *8*, 18. [CrossRef]
67. Garcia-Nicolas, M.; Ledesma-Escobar, C.A.; Priego-Capote, F. Spatial Distribution and Antioxidant Activity of Extracts from Citrus Fruits. *Antioxidants* **2023**, *12*, 781. [CrossRef]
68. Prathna, T.C.; Chandrasekaran, N.; Raichur, A.M.; Mukherjee, A. Biomimetic synthesis of silver nanoparticles by *Citrus limon* (lemon) aqueous extract and theoretical prediction of particle size. *Colloids Surf. B Biointerfaces.* **2011**, *82*, 152–159. [CrossRef] [PubMed]
69. Hasan, W.L.; Sari, R.; Hendradi, E. Green synthesis of antimicrobial silver nanoparticles using green tea extract: The role of concentration and pH. *J. Sains Farm. Klin.* **2024**, *11*, 25–31. [CrossRef]
70. Ildiz, N.; Korkmaz, F.; Yusufbeyoğlu, S.; Kilic, A.B.; Ocsoy, İ. Silver nanoparticles biosynthesized from *Vaccinium myrtillus* L. against multiple antibiotic resistance and biofilm forming *Escherichia coli* and *Pseudomonas aeruginosa*. *Indian J. Pharm. Educ. Res.* **2021**, *55*, 5220–5224. [CrossRef]
71. Cullity, B.D.; Stock, S.R. *Pearson. Elements of X-Ray Diffraction*, 3rd ed.; Pearson Education Limited: Harlow, UK, 2001.
72. Koch, W.; Kukula-Koch, W.; Komsta, Ł.; Marzec, Z.; Szwerc, W.; Głowniak, K. Green tea quality evaluation based on its catechins and metals composition in combination with chemometric analysis. *Molecules* **2018**, *23*, 1689. [CrossRef]
73. Minea, B.B.; Radulescu, C.; Dulama, I.D.; Banica, A.L.; Stirbescu, R.M.; Stanescu, S.G. Determination of heavy metals content from citrus fruit peels. *J. Sci. Arts* **2024**, *24*, 725–734. [CrossRef]
74. Rahim, M.; Saqib, N.U.; Wahid, F.; Khan, N.; Alrawi, L.I. Analysis of toxic heavy metal content of the most widely consumed fruits. *J. Phys. Sci.* **2020**, *31*, 61–73. [CrossRef]
75. Czech, A.; Zarycka, E.; Yanovych, D.; Zasadna, Z.; Grzegorczyk, I.; Kłys, S. Mineral content of the pulp and peel of various citrus fruit cultivars. *Biol. Trace Elem. Res.* **2020**, *193*, 555–563. [CrossRef] [PubMed]
76. Warczyk, A.; Gruba, P.; Józefowska, A.; Wanic, T.; Warczyk, A.; Świątek, B.; Pietrzykowski, M. Accumulation of heavy metals in blueberry (*Vaccinium myrtillus* L.) and dominant mosses (*Pleurozium schreberi* (Willd. ex Brid.) Mitt.) as bioindicators of the expressway influence on forest ecosystems. *Atmosphere* **2024**, *15*, 971. [CrossRef]
77. Safa, M.A.T.; Koohestani, H. Green synthesis of silver nanoparticles with green tea extract from silver recycling of radiographic films. *Results Eng.* **2024**, *21*, 101808. [CrossRef]
78. Tuoriniemi, J.; Johnsson, A.C.J.; Holmberg, J.P.; Gustafsson, S.; Gallego-Urrea, J.A.; Olsson, E.; Hassellöv, M. Intermethod comparison of the particle size distributions of colloidal silica nanoparticles. *Sci. Technol. Adv. Mater.* **2014**, *15*, 035009. [CrossRef]
79. Urcan, A.C.; Criste, A.D.; Szanto, K.I.; Ștefan, R.; Zahan, M.; Muscă, A.S.; Focsan, M.; Burtescu, R.F.; Olah, N.K. Antimicrobial and Antiproliferative Activity of Green Synthesized Silver Nanoparticles Using Bee Bread Extracts. *Pharmaceutics* **2023**, *15*, 1797. [CrossRef] [PubMed]
80. Padmanabhan, P.; Cheema, A.; Paliyath, G.; Caballero, B.; Finglas, P.M.; Toldrá, F. Berries and Related Fruits. In *Encyclopedia of Food and Health*; Academic Press: Oxford, UK, 2016; Volume 60, pp. 364–371.
81. Zuorro, A.; Iannone, A.; Natali, S.; Lavecchia, R. Green synthesis of silver nanoparticles using bilberry and red currant waste extracts. *Processes* **2019**, *7*, 193. [CrossRef]
82. Răut, I.; Constantin, M.; Șuică-Bunghez, R.; Firincă, C.; Alexandrescu, E.; Gîfu, I.C.; Doni, M.; Zamfir, L.-G.; Gurban, A.-M.; Jecu, L. Extracellular Biosynthesis, Characterization and Antimicrobial Activity of Silver Nanoparticles Synthesized by Filamentous Fungi. *J. Fungi* **2024**, *10*, 798. [CrossRef]
83. Verghese, R.J.; Mathew, S.K.; David, A. Antimicrobial activity of Vitamin C demonstrated on uropathogenic *Escherichia coli* and *Klebsiella pneumoniae*. *J. Curr. Res. Sci. Med.* **2017**, *3*, 88–93.
84. Abdelraheem, W.M.; Refaie, M.M.; Yousef, R.K.M.; Abd El Fatah, A.S.; Mousa, Y.M.; Rashwan, R. Assessment of antibacterial and anti-biofilm effects of vitamin C against Pseudomonas aeruginosa clinical isolates. *Front. Microbiol.* **2022**, *13*, 847449. [CrossRef]
85. Lapiz-Culqui, Y.K.; Meléndez-Mori, J.B.; Tejada-Alvarado, J.J.; Cortez, D.; Huaman, E.; Zarantes, V.M.N.; Oliva, M. Study of the physicochemical characteristics, antimicrobial activity, and in vitro multiplication of wild blackberry species from the Peruvian highlands. *Sci. Rep.* **2024**, *14*, 3863. [CrossRef] [PubMed]
86. Salah-Eldin, A.A.; Ibrahim, H.H.; Ali, M.R. Antimicrobial and therapeutic potentials of the blackberry extracts against Escherichia coli infection in male albino rats. *J. Sci. Food Agric.* **2024**, *104*, 7776–7787. [CrossRef] [PubMed]
87. Raza, S.; Wdowiak, M.; Grotek, M.; Adamkiewicz, W.; Nikiforow, K.; Mente, P.; Paczesny, J. Enhancing the antimicrobial activity of silver nanoparticles against ESKAPE bacteria and emerging fungal pathogens by using tea extracts. *Nanoscale Adv.* **2023**, *5*, 5786–5798. [CrossRef] [PubMed]

88. Loo, Y.Y.; Rukayadi, Y.; Nor-Khaizura, M.A.R.; Kuan, C.H.; Chieng, B.W.; Nishibuchi, M.; Radu, S. In vitro antimicrobial activity of green synthesized silver nanoparticles against selected gram-negative foodborne pathogens. *Front. Microbiol.* **2018**, *9*, 1555. [CrossRef]
89. Duran, N.; Duran, M.; De Jesus, M.B.; Seabra, A.B.; Favaro, W.J.; Nakazato, G. Silver nanoparticles: A new view on mechanistic aspects on antimicrobial activity. *Nanomed. Nanotechnol. Biol. Med.* **2016**, *12*, 789–799. [CrossRef]
90. Pal, S.; Tak, Y.K.; Song, J.M. Does the antibacterial activity of silver nanoparticles depend on the shape of the nanoparticle? A study of the gram-negative bacterium *Escherichia coli*. *Appl. Environ. Microbiol.* **2007**, *73*, 1712–1720. [CrossRef]
91. Li, W.R.; Xie, X.B.; Shi, Q.S.; Zeng, H.Y.; Ou-Yang, Y.S.; Chen, Y.B. Antibacterial activity and mechanism of silver nanoparticles on *Escherichia coli*. *Appl. Environ. Microbiol.* **2010**, *85*, 1115–1122. [CrossRef]
92. Ansari, M.A.; Khan, H.M.; Khan, A.A.; Ahmad, M.K.; Mahdi, A.A.; Pal, R.; Cameotra, S.S. Interaction of silver nanoparticles with *Escherichia coli* and their cell envelope biomolecules. *J. Basic Microbiol.* **2014**, *54*, 905–915. [CrossRef]
93. Kim, J.S.; Kuk, E.; Yu, K.N.; Kim, J.H.; Park, S.J.; Lee, H.J.; Jeong, D.H.; Cho, M.H. Antimicrobial effects of silver nanoparticles. *Nanomed. Nanotechnol. Biol. Med.* **2007**, *3*, 95–101. [CrossRef]

Disclaimer/Publisher's Note: The statements, opinions and data contained in all publications are solely those of the individual author(s) and contributor(s) and not of MDPI and/or the editor(s). MDPI and/or the editor(s) disclaim responsibility for any injury to people or property resulting from any ideas, methods, instructions or products referred to in the content.